

# A Green Coordinated Multi-Cell NOMA System with Fuzzy Logic Based Multi-Criterion User Mode Selection and Resource Allocation

Haiyong Zeng, *Student Member, IEEE*, Xu Zhu, *Senior Member, IEEE*, Yufei Jiang, *Member, IEEE*, Zhongxiang Wei, *Member, IEEE*, and Tong Wang, *Member, IEEE*

**Abstract**—We consider a multi-cell non-orthogonal multiple access (NOMA) system with coordinated base stations (BSs) and investigate its downlink user coordination mode selection and resource allocation to green the system while maintaining high spectral efficiency, in the presence of inter-cell interference. To the best of our knowledge, this is the first work to consider multiple criteria in user coordination mode selection for coordinated NOMA systems, and a fuzzy logic (FL) based approach is proposed to balance among multiple criteria to achieve higher robustness against the combined effect of shadowing, fading and inter-cell interference, compared to the previous single-criterion based user coordination mode selection methods. This is also the first known effort to investigate multi-subchannel resource allocation for coordinated NOMA where the previous work on coordinated orthogonal multiple access is not applicable. Two resource allocation algorithms are proposed: a) a serving channel gain based subchannel allocation (SCG-SA) algorithm, based on the theoretical proof that the total transmission power is mono-decreasing with respect to the SCG of the non-coordinated user in each cell with the highest channel gain on the shared subchannel; b) a low-complexity FL user ranking order based joint resource allocation (FLURO-JRA) algorithm, which requires no separate user ranking process in subchannel allocation, thanks to the FL ranking list generated from user coordination mode selection. Also, the effects of imperfect channel state information and successive interference cancellation are considered. Numerical results show that the proposed multi-criterion based schemes significantly outperform the previous schemes based on single-criterion user coordination mode selection, in terms of transmission power and energy efficiency (EE), contributing to a greener system.

**Index Terms**—Non-orthogonal multiple access, fuzzy logic, resource allocation, user mode selection, energy efficiency, coordination.

## I. INTRODUCTION

Non-orthogonal multiple access (NOMA) [1]–[3], which allows multiple users to share the same frequency-domain,

Manuscript received September 14, 2018; revised January 19, 2019; accepted March 6, 2019. (Corresponding author: Xu Zhu.)

This work was supported in part by the Department for DCMS, UK, through the Liverpool 5G Project, in part by the Science and Technology Innovation Commission of Shenzhen under Grants No. JCYJ20170307151258279 and No. JCYJ20180306171800589, in part by the Natural Science Foundation of Guangdong Province under Grants No. 2018A030313298 and No. 2018A030313344, and in part by the Natural Science Foundation of China under Grant No. 61801145.

Part of this work was presented at the IEEE Globecom 2018.

H. Zeng, Y. Jiang and T. Wang are with the School of Electronic and Information Engineering, Harbin Institute of Technology, Shenzhen, China.

X. Zhu is with the University of Liverpool, Liverpool, UK. (e-mail: xuzhu@liverpool.ac.uk)

Z. Wei is with the University College London, London, UK.

time-domain, or code-domain resource element, has been envisioned as a promising technology for the fifth generation (5G) wireless communication networks due to its higher achievable spectral efficiency than conventional orthogonal multiple access (OMA) techniques. Recently, a number of NOMA techniques have been studied, including power-domain NOMA [4]–[6], low-density spreading (LDS) [7], pattern division multiple access (PDMA) [8], multi-user shared access (MUSA) [9], sparse code multiple access (SCMA) [10] and lattice partition multiple access (LPMA) [11]. By exploiting power-domain multiplexing and successive interference cancellation (SIC), power-domain NOMA allows receivers to decode and demodulate the superposition of the encoded signals [12]–[15], and is regarded as optimal from the view of reaching the corresponding capacity region of downlink broadcast channel [1].

In a more practical scenario, *i.e.*, multi-cell power-domain NOMA, the users located at edge of cells generally suffer from poor channel condition and strong inter-cell interference. In order to achieve the targeted quality of service (QoS), more transmission power is required for cell-edge users, which is not power efficient and causes stronger multi-cell interference [16]–[18]. To alleviate this, coordination techniques between base stations (BSs), such as coordinated multi-point (CoMP) with joint transmission, can be utilized to allow joint signal processing for the cell-edge users [19]–[22]. It has been demonstrated in [23] and [24] that the network with coordinated BSs can benefit from the distributed space diversity, where distributed BSs transmit signals to corresponding cell-edge users at the same time. In [23], Choi firstly proposed a joint transmission NOMA scheme in a coordinated network with two cells. In [24], it was shown that the coordinated NOMA outperforms the non-coordinated NOMA system, and the coordinated OMA system.

It is worthy noting that user coordination mode selection is essential for multi-cell coordination, both for OMA and NOMA [25]–[31]. In [27], novel user scheduling and power allocation algorithms were proposed to improve the energy-efficiency (EE) for coordinated OMA systems. As NOMA is expected to support much more users than OMA, compared to the conventional OMA-based coordination techniques [25]–[27], the coordination mode selection of each user plays a more important role in enhancing the system performance and achieving green communication for coordinated NOMA systems [28]–[31]. Current user coordination mode selection approaches for coordinated NOMA systems can be mainly

categorized into two types: a) the approaches based on the distance from a user to an adjacent BS [28] [29]; b) the approaches based on the channel gain between each user and an adjacent BS [30] [31]. The authors of [28] proposed an EE-oriented power allocation scheme for coordinated NOMA, in which the users are selected to be in coordination mode based on their distances. However, they merely considered the single-channel power allocation and paid little attention to the multi-subchannel case. In [30], an opportunistic NOMA scheme was proposed to enhance the network capacity in a coordinated system, and the coordinated users are selected based on channel gain. However, the user mode selection approaches based on distance are sensitive to fading and shadowing, while the performance of the approaches based on channel gain can be severely affected by channel state information (CSI) estimation and inter-cell interference.

As mentioned above, the single-criterion based user coordination mode selection methods generally lead to poor system performance, and are sensitive to multiple varying parameters, such as fading, shadowing and inter-cell interference. To this end, multiple criteria are necessary for user coordination mode selection to enhance the robustness. Fuzzy logic (FL) is an effective artificial intelligence (AI) approach to make a comprehensive and reasonable decision based on multiple input parameters [32] [33]. As mentioned in [33], FL has been applied to wireless communications to offer flexibility and superior performance in terms of channel estimation, handover, interference management, *etc.* In [34], an iterative fuzzy tracking method was applied to track channel coefficients. In [35], FL was employed for handover in self-organizing networks. The authors of [36] proposed a game theory and FL inference system based self-optimized power allocation algorithm. Hence, it is beneficial to investigate employing an FL based multi-criterion scheme for user coordination mode selection in coordinated NOMA systems.

In coordinated NOMA systems, the performance is largely influenced by resource allocation including subchannel assignment and power allocation. Since multiple users can share the same subchannel in coordinated NOMA, the previous work on resource allocation for coordinated OMA systems [17] [19] [27] may not be utilized directly. The work in [28] and [30] has focused on power allocation only for multi-cell coordinated NOMA, assuming a single-channel model. Also, the previous work on coordinated NOMA [28]–[31] has assumed perfect CSI and SIC, which is not practical. The subchannel allocation for coordinated NOMA still remains an open challenge in the literature.

Motivated by the above open issues, we consider a multi-cell downlink coordinated power-domain NOMA system, where each user is dynamically selected by FL to work in two modes: a) non-coordinated mode with only one serving BS; b) coordinated mode with multiple serving BSs. Low-complexity resource allocation is also investigated alongside user coordination mode selection to green the system. The contributions of this paper are summarized as follows:

1) To the best of our knowledge, this is the first work to consider multiple criteria (distance, received signal strength and inter-cell interference) for user coordination mode selection

in coordinated NOMA systems. We take the reference signal received power (RSRP) of each user to indicate their received signal strength, and the variance of RSRP to indicate the level of inter-cell interference. To balance among the multiple criteria, we propose an FL based scheme where the user with higher FL output coordination suitability is more likely to be chosen in the coordinated mode. The proposed FL based multi-criterion scheme is more robust against fading, shadowing and inter-cell interference than the previous single-criterion based user mode selection schemes [28] [30], with significantly higher performance in terms of transmission power and EE.

2) To the best of our knowledge, this is the first work to investigate multi-subchannel resource allocation for coordinated NOMA systems, alongside our user coordination mode selection scheme. The previous work either assumed a single-channel model for coordinated NOMA [28]–[31] or was aimed for resource allocation of coordinated OMA [17] [19] [27], which may not be utilized for coordinated NOMA directly. Besides, signal processing in the presence of imperfect CSI estimation and SIC is investigated, which is more practical. An intensive analysis is provided to theoretically prove that the transmission power consumption is mono-decreasing with respect to the serving channel gain (SCG) of the non-coordinated user in each cell with the highest channel gain on the shared SC. In light of this, an SCG based subchannel allocation (SCG-SA) algorithm is proposed. Also, a closed-form solution to optimal power allocation is derived.

3) We conduct the first study of joint optimization of subchannel and power allocation for coordinated NOMA systems, and propose an FL user ranking order based joint resource allocation (FLURO-JRA) algorithm. As user ranking plays a dominant role in the complexity of subchannel assignment [5] [6], we feed the FL output ranking list directly to subchannel assignment, which saves tremendous complexity over the previous work that requires a dedicated user ranking process in subchannel assignment. The FLURO-JRA algorithm also outperforms the two-step SCG-SA algorithm in terms of EE and transmission power consumption, contributing to a greener coordinated NOMA system.

The rest of this paper is organized as follows. The coordinated NOMA system model and optimization problem are formulated in Section II. Section III introduces the FL based multi-criterion user coordination mode selection scheme. The SCG based subchannel assignment and power allocation algorithms are proposed in Section IV. Section V proposes the low-complexity FLURO-JRA algorithm to jointly optimize the subchannel and power allocation. Numerical results of the proposed algorithms are presented and discussed in Section VI. Finally, Section VII concludes this paper.

*Notations:* A set of frequently used notations in this paper are listed in Table I.

## II. SYSTEM MODEL AND PROBLEM FORMULATION

### A. System Model

We consider a downlink multi-cell NOMA system with  $B$  BSs and  $K$  users. Assume that the overall bandwidth

TABLE I  
SET NOTATIONS

$S_{n,b}$	The set of users served by BS $b$ on SC $n$
$B_k$	The set of coordinated BS(s) serving for user $k$
$S_{n,b,k}$	The set of users on SC $n$ that are served by BS $b$ and have higher channel gain than user $k$ , when user $k$ is in the coordinated mode
$\tilde{S}_{n,B_k,k}$	The set of users on SC $n$ that are served by BS $B_k$ and have higher channel gain than user $k$ , when user $k$ is in the non-coordinated mode

of the coordinated NOMA system  $W$  is divided uniformly into  $N$  subchannels (SCs), and each BS transmits signals to its user set through these SCs. As depicted in Fig. 1, in order to improve performance, these users are selected to work in two modes: a) non-coordinated mode with only one serving BS; b) coordinated mode with multiple coordinated BSs. The coordinated BSs are connected to a centralized controller through high-capacity links (e.g., optical fiber). User coordination mode selection and resource allocation are performed at the centralized controller [19]–[22].

According to NOMA principle [4], multiple users can share the same SC. Let  $x_{k,n} \in \{0, 1\}$ , in which  $x_{k,n} = 1$  indicates that user  $k$  is allocated to SC  $n$ . Define  $S_{n,b}$  as the set of users served by BS  $b$  ( $b = 1, \dots, B$ ) on SC  $n$  ( $n = 1, \dots, N$ ). The symbol  $m_{b,n}$  transmitted by BS  $b$  on SC  $n$  is given by

$$m_{b,n} = \sum_{k \in S_{n,b}} \sqrt{p_{k,n}} D_{k,n}, \quad (1)$$

where  $p_{k,n}$  denotes the transmission power allocated to user  $k$  on SC  $n$  and  $D_{k,n}$  is the data symbol with unit energy.

In Fig. 1, the channel frequency response from BS  $b$  to user  $k$  on SC  $n$  is denoted by  $h_{b,k,n}$ . Denote  $\hat{h}_{b,k,n}$  as the estimated of  $h_{b,k,n}$ , with estimation error  $e_{b,k,n} = h_{b,k,n} - \hat{h}_{b,k,n}$ , which can be regarded as an independent zero-mean complex Gaussian random variable with variance  $\sigma_{\text{error}}^2$ .  $h_{b,k,n}$  is independent of  $e_{b,k,n}$  [37].

Let  $B_k$  denote the set of coordinated BS(s) serving for user  $k$ . The received signal at user  $k$  on SC  $n$  can be written as

$$y_{k,n} = \sum_{b \in B_k} \left( \hat{h}_{b,k,n} + e_{b,k,n} \right) m_{b,n} + z_{k,n} + \sum_{b \in \{B/B_k\}} \left( \hat{h}_{b,k,n} + e_{b,k,n} \right) m_{b,n}, \quad (2)$$

where  $z_{k,n}$  stands for the additional white complex Gaussian noise  $z_{k,n} \sim \mathbb{C}N(0, \sigma_n^2)$ , with  $\sigma_n^2$  as the variance on SC  $n$ .

Substituting Eq. (1) into Eq. (2), yields

$$y_{k,n} = \sum_{b \in B_k} \left( \hat{h}_{b,k,n} + e_{b,k,n} \right) \left( \sqrt{p_{k,n}} D_{k,n} + \sum_{i \in S_{n,b}, i \neq k} \sqrt{p_{i,n}} D_{i,n} \right) + \sum_{b \in \{B/B_k\}} \left( \hat{h}_{b,k,n} + e_{b,k,n} \right) \sum_{i \in S_{n,b}} \sqrt{p_{i,n}} D_{i,n} + z_{k,n}. \quad (3)$$

Define  $H_{b,k,n} = |h_{b,k,n}|^2$  as the true channel gain of user  $k$  on SC  $n$ , and  $\hat{H}_{b,k,n} = |\hat{h}_{b,k,n}|^2$  as the estimated channel

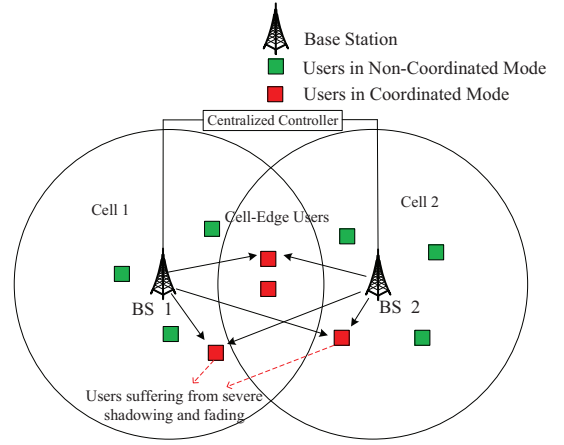


Fig. 1. System model of multi-cell coordinated NOMA.

gain, we have

$$H_{b,k,n} = \hat{H}_{b,k,n} + E_{b,k,n}, \quad (4)$$

where  $E_{b,k,n} = |e_{b,k,n}|^2 + 2|\hat{h}_{b,k,n}||e_{b,k,n}|$  is due to the imperfect CSI estimation of user  $k$ .

At the receiver, SIC process is conducted to decode and demodulate the received signals. According to the NOMA protocol, the optimal order in SIC decoding is the increasing order of channel gains [4]. On the basis of this order, any user can successfully demodulate and remove the signals from the other users with smaller channel gain. Due to imperfect SIC process, there exists residual power of the previously decoded users with lower channel gain, which causes error propagation [38]. Based on the principle of NOMA, for NOMA users  $i$  and  $j$  in the same group, their transmission power  $p_{i,n}$  and  $p_{j,n}$  on SC  $n$  should satisfy  $p_{i,n} < p_{j,n}$ , if the estimated channel gain of user  $i$  is higher than that of user  $j$ .

1) *Users in the Coordinated Mode:* As mentioned above, in order to improve system performance, the users can be selected to work in the coordinated or non-coordinated mode. Let  $K_C$  denote the number of the coordinated users in the system.

On one hand, if user  $k$  is in the coordinated mode, the set of coordinated BSs serving for user  $k$  is  $B_k$ . Assume that the messages sent to user  $k$  by  $B_k$  share the same transmit power [28]. Denote the power of intra-cell and inter-cell interference for user  $k$  as  $I_{k,n}$  and  $\varphi_{k,n}$ , respectively. Due to the coordination between BSs [19]–[22], the inter-cell interference of user  $k$  from the coordinated BSs  $B_k$  is eliminated, and the inter-cell interference is merely from the set of BSs  $B/B_k$ .

Based on Eq. (3), due to the coordination between BSs and SIC process, the power of intra-cell and inter-cell interference for coordinated user  $k$  can be respectively obtained, as

$$I_{k,n} = \sum_{b \in B_k} \left( \hat{H}_{b,k,n} + E_{b,k,n} \right) \sum_{i \in S_{n,b,k}} p_{i,n} + \omega_k \sum_{b \in B_k} \left( \hat{H}_{b,k,n} + E_{b,k,n} \right) \sum_{i \in \{S_{n,b}/S_{n,b,k}\}} p_{i,n}, \quad (5)$$

$$\varphi_{k,n} = \sum_{b \in \{B/B_k\}} \left( \hat{H}_{b,k,n} + E_{b,k,n} \right) \sum_{i \in S_{n,b}} p_{i,n}, \quad (6)$$

where  $S_{n,b,k} = \left\{ \tilde{k} \mid \hat{H}_{b,\tilde{k},n} \geq \hat{H}_{b,k,n}, \tilde{k} \in S_{n,b} \right\}$  denotes the set of users on SC  $n$  that are served by BS  $b$  and have higher channel gain than coordinated user  $k$ , and  $\omega_k$  is the proportion of SIC residual power from user  $k$  ( $0 \leq \omega_k \leq 1$ ) [38]. Note that if  $B_k = B$ , i.e., the coordinated user  $k$  is served by all  $B$  BSs. We have  $\varphi_{k,n} = 0$ , which means that the inter-cell interference of user  $k$  is eliminated [28].

After SIC, the received signal-to-interference-plus-noise ratio (SINR) for coordinated user  $k$  on SC  $n$  is given by

$$\gamma_{k,n} = \frac{\sum_{b \in B_k} \hat{H}_{b,k,n} p_{k,n}}{\sum_{b \in B_k} E_{b,k,n} p_{k,n} + I_{k,n} + \varphi_{k,n} + \sigma_n^2}, \quad (7)$$

where the term  $\sum_{b \in B_k} E_{b,k,n} p_{k,n}$  denotes the noise due to imperfect CSI estimation. As a result, the achievable data rate (in bps/Hz) of the coordinated user  $k$  on SC  $n$  is given by

$$R_{k,n} = C_k \log_2(1 + \gamma_{k,n}), \quad (8)$$

where  $C_k \in \{0, 1\}$ . Explicitly,  $C_k = 1$  indicates user  $k$  is in the coordinated mode, otherwise user  $k$  is in the non-coordinated mode.

2) *Users in the Non-Coordinated Mode:* On the other hand, if user  $k$  is selected to work in the non-coordinated mode (i.e.,  $C_k = 0$ ), the number of serving BS is reduced to one. Then, the power of intra-cell interference  $\tilde{I}_{k,n}$  and inter-cell interference  $\tilde{\varphi}_{k,n}$  can be expressed as

$$\begin{aligned} \tilde{I}_{k,n} &= \left( \hat{H}_{B_k,k,n} + E_{B_k,k,n} \right) \sum_{i \in \{\tilde{S}_{n,B_k,k}\}} p_{i,n} + \\ \omega_k \left( \hat{H}_{B_k,k,n} + E_{B_k,k,n} \right) &\sum_{i \in \{S_{n,B_k}/\tilde{S}_{n,B_k,k}\}} p_{i,n}, \end{aligned} \quad (9)$$

$$\tilde{\varphi}_{k,n} = \sum_{b \in \{B \setminus B_k\}} \left( \hat{H}_{b,k,n} + E_{b,k,n} \right) \sum_{j \in \{S_{n,b}\}} p_{j,n}, \quad (10)$$

where  $\tilde{S}_{n,B_k,k} = \left\{ \tilde{k} \mid \hat{H}_{b,\tilde{k},n} \geq \hat{H}_{B_k,k,n}, \tilde{k} \in S_{n,B_k} \right\}$  stands for the set of users on SC  $n$  that are served by BS  $B_k$  and have higher channel gain than non-coordinated user  $k$ . Following [28], we consider there is only one coordinated user served by the coordinated BSs on SC  $n$ . Based on Eq. (9) and Eq. (10), when user  $k$  is in the non-coordinated mode, the SINR for user  $k$  on SC  $n$  is given by

$$\tilde{\gamma}_{k,n} = \frac{\hat{H}_{B_k,k,n} p_{k,n}}{E_{B_k,k,n} p_{k,n} + \tilde{I}_{k,n} + \tilde{\varphi}_{k,n} + \sigma_n^2}. \quad (11)$$

The achievable data rate on SC  $n$  can be expressed as

$$R_{k,n} = (1 - C_k) \log_2(1 + \tilde{\gamma}_{k,n}). \quad (12)$$

The overall data rate of user  $k$  is  $R_k = \sum_{n=1}^N R_{k,n}$ .

*Remark 1:* For multi-cell coordinated NOMA systems, the users located in the edge of cells generally suffer from poor channel conditions and strong inter-cell interference. Also, the users close to the serving BS who suffer severe fading and shadowing, have poor channel conditions. To improve

performance, these users are chosen in the coordinated mode and served by a set of coordinated BSs.

*Remark 2:* The user coordination mode can be selected by a single criterion (e.g., distance [28] or channel gain [30]) based method, or the FL based multi-criterion user mode selection scheme proposed in Section III.

## B. Problem Formulation

In this subsection, we dedicate to minimizing the total transmission power under certain QoS requirements. Let  $\mathbf{X} = [x_{k,n}]_{K \times N}$  denote the subchannel assignment matrix,  $\mathbf{C} = [C_k]_{K \times 1}$  be the user coordination mode selection matrix, and  $\mathbf{P} = [p_{k,n}]_{K \times N}$  be the power allocation matrix, respectively.

The total transmission power  $P_t$  is expressed as

$$P_t = \sum_{n=1}^N \sum_{b=1}^B \sum_{k \in S_{n,b}} p_{k,n}. \quad (13)$$

Therefore, the optimization problem for the downlink multi-cell coordinated NOMA system can be formulated as

$$\min_{\mathbf{P}, \mathbf{X}, \mathbf{C}} P_t \quad (14)$$

subject to

$$(C1) : x_{k,n} \in \{0, 1\},$$

$$(C2) : C_k \in \{0, 1\},$$

$$(C3) : \sum_{k \in S_{n,b}} x_{k,n} = L,$$

$$(C4) : R_k \geq R_{\min},$$

$$(C5) : p_{k,n} \geq 0,$$

$$(C6) : \text{if } \hat{H}_{b,i,n} > \hat{H}_{b,j,n}, \text{ then } p_{i,n} < p_{j,n}, \\ \forall i, j \in S_{n,b}, b = 1, \dots, B, n = 1, \dots, N,$$

where (C4) is the users' QoS requirements constraint, with  $R_{\min}$  denoting the minimum rate requirement, (C3) constrains the maximum number of allocated users sharing the same SC for each BS, and (C6) indicates that the signal from the user with lower channel gain can be decoded by the user with higher channel gain. Consequently, the EE of the coordinated NOMA system is given by  $E = \sum_{k=1}^K R_k / (P_t + BP_c)$ , with  $P_c$  denoting the circuit power of each BS. Note that  $L$  makes a trade-off between performance and complexity. The implementation complexity of SIC at receiver side increases with  $L$  [5].

## C. Overall Algorithms Description

Due to the non-convex constraint of users' rates in (C4) and the binary integer assignment variables in (C1), (C2), the considered resource allocation problem in Eq. (14) is difficult to solve. It is very challenging to obtain the global optimal resource allocation solution in polynomial time. Hence, to strike an attractive balance between the performance and complexity, we divide Eq. (14) into three subproblems, namely user coordination mode selection, subchannel assignment and

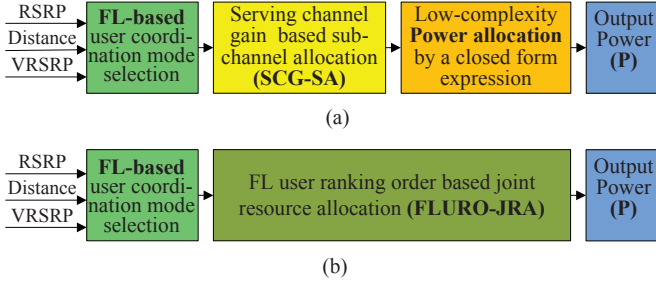


Fig. 2. Block diagram of (a) FL-based user mode selection, SCG-SA and power allocation algorithms and (b) FL-based user mode selection and FLURO-JRA algorithm for coordinated NOMA systems.

power allocation, to obtain low-complexity and effective near-optimal solutions. The block diagram of the proposed algorithms is depicted in Fig 2.

The proposed algorithms are expected to run in every time slot at the centralized controller. To execute the proposed algorithms, physical layer parameters (*e.g.*, distance, CSI and RSRP) are collected at BSs and sent to the centralized controller through backhaul links [19] [27]. The centralized controller feeds back the optimal resource allocation indicators (user mode selection, subchannel assignment and transmit power policy for each BS and subchannel) to the BSs. It is worth noting that, the incurred overhead for describing these parameters are all typically of a level of a few bits [39], which can be embedded into standard size of frame. Hence, these algorithms are applicable to coordinated NOMA systems.

### III. FUZZY LOGIC BASED MULTI-CRITERION USER COORDINATION MODE SELECTION

For multi-cell coordinated NOMA systems, the users located near to cell edge generally have poor channel gains and strong inter-cell interference. In addition, due to the effect of fading and shadowing, some cell-center users also suffer from poor channel conditions. Hence, it is significant to determine which users are in coordinated mode or non-coordinated mode. Two kinds of user coordination mode selection methods are mostly mentioned in literatures: distance based [28] [29] and channel gain based methods [30] [31]. Generally, the two user selection methods can be respectively expressed, as

$$\begin{aligned} \text{if } d_k > d_{\text{thd}}, \text{ user } k \text{ is in the coordinated mode,} \\ \text{if } H_k < H_{\text{thd}}, \text{ user } k \text{ is in the coordinated mode,} \end{aligned}$$

where  $d_{\text{thd}}$  and  $H_{\text{thd}}$  are predetermined thresholds. Nevertheless, these methods based on a single threshold only divide users into the coordinated and non-coordinated groups. Given a large number of coordinated users, the majority of frequency resource will be assigned to the coordinated users, which ignores the fairness among the users. Hence, the threshold should be adaptively changed when the number of coordinated users is limited. The other effective scheme is to perform a ranking based user coordination mode selection. Based on a ranking criterion (*e.g.*, distance or channel gain), users are sorted in order and some top users are chosen as the coordinated users.

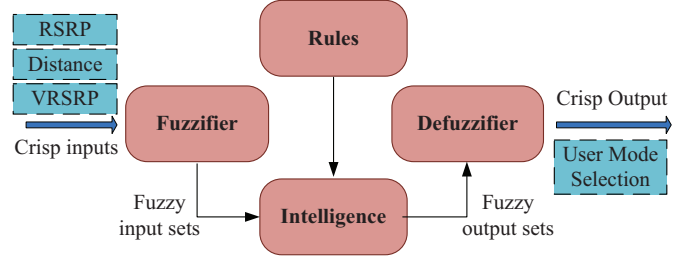


Fig. 3. Structure of the FL based multi-criterion user coordination mode selection scheme.

However, as an empirical user mode selection criterion, the performance of the distance based user mode selection method is sensitive to fading and shadowing. Due to the CSI estimation error and inter-cell interference, the channel gain based approaches cannot provide enough information in consideration of system performance. As a result, some users' coordination mode cannot be selected appropriately, which decreases the system performance. As mentioned in [33], FL has been applied for wireless communication areas due to its flexibility and superior performance. Therefore, to combat fading, shadowing and inter-cell interference effects, we propose an FL based multi-criterion user coordination mode selection scheme to balance among distance, RSRP and inter-cell interference. The block design for the proposed FL based user mode selection scheme is shown in Fig. 3, where a fuzzifier module transforms the crisp inputs into linguistic variables (fuzzy sets) by using fuzzy membership functions, then the rules are used to map input sets to output sets, and finally the output sets are transformed to a crisp output by a defuzzifier module [33].

#### A. Fuzzy Inputs

For each user  $k$ , the distance  $d_k$  and RSRP between the user and the serving BS are two of inputs of proposed FL scheme. As we know, RSRP is the received signal strength indicator. In addition, considering the effect of inter-cell interference, we choose the variance of RSRP (VRSRP) to be the other potential input. It is valid to assume that the strongest RSRP is from the user's potential coordinated BS. If the RSRPs are close to each other, the user is more likely in stronger inter-cell interference area. Hence, VRSRP is selected as one criterion. User with lower VRSRP has a higher probability to be chosen in the coordinated mode. The VRSRP of user  $k$  is given by

$$V_{\text{RSRP},k} = E \left[ (\text{RSRP}_k^b - \overline{\text{RSRP}}_k)^2 \right], \quad (15)$$

where  $\text{RSRP}_k^b$  denotes the RSRP of user  $k$  from an adjacent BS  $b$ , and  $\overline{\text{RSRP}}_k$  is the mean value of RSRPs from user  $k$ 's potential coordinated cells. Combining the three criteria by FL can improve the effectiveness of user coordination mode selection.

#### B. Fuzzification Process

In order to perform the fuzzification process, three inputs and one outputs should be mapped to fuzzy sets, the name of

TABLE II  
COORDINATION SUITABILITY LIST

No.	Criteria			Coordination Suitability
	VRSRP	D	RSRP	
1	small	short	bad	medium
2	small	short	medium	bad
3	small	short	good	very bad
4	small	medium	bad	good
5	small	medium	medium	medium
6	small	medium	good	medium
7	small	large	bad	very good
8	small	large	medium	very good
9	small	large	good	good
10	medium	short	bad	medium
11	medium	short	medium	bad
12	medium	short	good	very bad
13	medium	medium	bad	good
14	medium	medium	medium	medium
15	medium	medium	good	bad
16	medium	large	bad	very good
17	medium	large	medium	good
18	medium	large	good	medium
19	large	short	bad	bad
20	large	short	medium	bad
21	large	short	good	very bad
22	large	medium	bad	medium
23	large	medium	medium	bad
24	large	medium	good	very bad
25	large	large	bad	good
26	large	large	medium	medium
27	large	large	good	bad

which are as follows.

$$\begin{aligned}
 X &= \text{VRSRP} \in \{\text{small, medium, large}\}, \\
 Y &= d \in \{\text{short, medium, long}\}, \\
 Z &= \text{RSRP} \in \{\text{bad, medium, good}\}, \\
 O &= \text{output} \in \{\text{very bad, bad, medium, good, very good}\}.
 \end{aligned}$$

The fuzzy output set indicates the user's suitability for the coordinated mode in consideration of all three inputs. Fig. 4 presents the FL membership degree of three inputs and output. Since all three inputs change linearly and continuously, the Trapezoidal function is chosen to generate membership function [33].

For one input, membership function generates one membership degree which is between 0 to 1, according to the type (small/medium/large *etc.*) of input. As there is no experience information of RSRP and VRSRP, their memberships have balanced distribution of three levels. Note that the membership function for the distance is not symmetric for that generally the coordinated users located in the edge area of cells, as a result that its distribution of levels skews to right. Users with short distance to cell center have lower probability to be selected in the coordinated mode. Therefore, as depicted in Fig 4, the part which represents "short" is larger than "medium" and "long", which ensure that fewer center users are switched to the coordinated mode. The medium level of membership of fuzzy output has more core area, which makes weights of side levels closer to edges and enlarges difference of suitability of the coordinated and non-coordinated users.

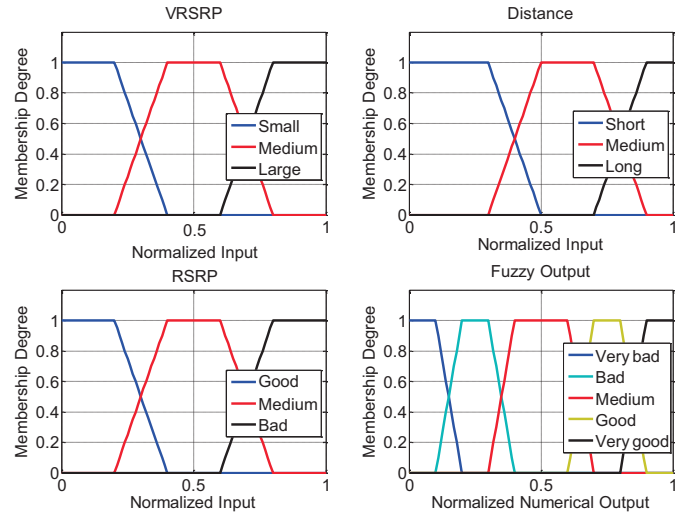


Fig. 4. Fuzzy membership functions of three inputs and output.

### C. Defuzzification Process

As presented in Table II, with three 3-level inputs, we formulate 27 FL rules to map three inputs to output. This fuzzy rule base indicates different outputs with 27 points of view on inputs. If two or more inputs are at same level, the output is set to same level. If all inputs are at different level, the output is set to medium level. Since FL rules are set by AND logic, the membership of FL output set can be obtained by taking the minimum value of the inputs

$$\mu_o \triangleq \min(\mu_X, \mu_Y, \mu_Z), \quad (16)$$

where  $\mu_X, \mu_Y$  and  $\mu_Z$  denote the degree of membership of VRSRP, distance and RSRP, respectively.

From Eq. (16), a fuzzy output membership set, consisting of 27 elements on inputs, is generated. In order to compare fuzzy output of different users, we have to map the output membership set to a crisp numerical output. In this paper, we utilize the weighted average defuzzification method [33] to transform the aggregated output set  $\mu_o$  into a crisp number. The crisp number, which is between  $[0, 1]$  and indicates user's suitability for the coordinated mode, can be obtained as

$$\eta = \frac{\sum(\mu_o \cdot O_M(\mu_o))}{\sum \mu_o}, \quad (17)$$

where  $O_M(\mu_o)$  denotes the middle value of the normalized numerical value of output membership  $\mu_o$ , and the user with larger  $\eta$  has more probability to be chosen in the coordinated mode.

After the FL output crisp number of all  $K$  users have been obtained, we rank the users in descending order based on  $\eta$  and form a FL output ranking list  $\Gamma_{FL}$ . Then, we choose the top  $K_C$  users in  $\Gamma_{FL}$  to work in the coordinated mode, and the rest users are selected in the non-coordinated mode. It is worth noting that the proposed FL based multi-criterion user coordination mode selection algorithm is widely applicable to various NOMA systems including power-domain, code-domain and multi-domain NOMA, as well as OMA systems.

#### IV. SERVING CHANNEL GAIN BASED SUBCHANNEL ALLOCATION AND POWER ALLOCATION

In this section, we investigate effective resource allocation algorithms in multi-cell coordinated NOMA systems to minimize the transmission power consumption. Based on *Theorem 1*, we propose an SCG based subchannel allocation algorithm. By transforming the non-convex power allocation problem into a convex form, a closed-form expression of optimal power allocation is derived.

As mentioned above, for each BS (e.g., BS  $b$ ),  $L$  users can be simultaneously multiplexed on a SC, i.e., there are  $L - 1$  non-coordinated users served by BS  $b$  to share the same SC with one coordinated user. Following [5], as there are  $N$  SCs, we assume that the number of users served by each BS  $b$  is  $K_b = LN$ , with the number of coordinated users served by coordinated BSs being  $K_C = N$ . For each BS, since the coordinated users usually suffer from poor channel conditions, they are taken as weak users compared to the non-coordinated users, and the interference from the coordinated users can be decoded and removed by the non-coordinated users on the same subchannel. For a non-coordinated user  $k$  allocated to SC  $n$ , considering the imperfect channel estimation, define the SCG of user  $k$  as  $B_k$  on SC  $n$   $\hat{H}_{b,k,n}$ . Similarly, for a coordinated user  $j$  on SC  $n$ , since it is served by multiple coordinated BSs, its SCG is  $\sum_{b \in B_k} \hat{H}_{b,j,n}$ .

##### A. SCG Based Subchannel Allocation

According to Eq. (11), the performance of non-coordinated user  $k$  gets better as its SCG  $\hat{H}_{b,k,n}$  is increased. Nevertheless, in multi-cell coordinated NOMA systems, increasing SCG of user  $k$  inevitably effects the intra-cell and inter-cell interference of other users sharing the same SC, as well as the power allocation among users. Unfortunately, there is little analysis at present to theoretically explore the effect of the non-coordinated users' SCG on the transmission power overhead in multi-cell coordinated NOMA systems. Hence, it is significant to make a theoretical discussion on the relationship between the increasing SCG of non-coordinated users and the variation of total transmission power consumption.

*Theorem 1:* In multi-cell coordinated NOMA systems, with relatively low channel estimation error and SIC error, the total transmission power consumption  $P_t$  is mono-decreasing with respect to the SCG of the non-coordinated user in each cell with the highest channel gain on the shared SC.

Specially, when  $L = 2$ , since the number of non-coordinated user on each SC for each cell is one,  $P_t$  is mono-decreasing with respect to the SCG of an arbitrary non-coordinated user.

*Proof of Theorem 1:* See Appendix A.

According to *Theorem 1*, the network transmission power continues to decrease with respect to the increasing of SCG of the non-coordinated user in each cell with the highest channel gain on the shared SC. The mono-decreasing property of overall transmission power consumption with respect to the SCG of non-coordinated user for multi-cell coordinated NOMA systems is also illustrated in Fig. 12.

---

#### Algorithm 1 SCG-SA for the Non-Coordinated Users in Cell $b$

---

**Require:** Given the  $N \times K_{N_b}$  allocated list  $S_{\text{alloc}} = \mathbf{0}$  to record the non-coordinated users assigned to SC  $n$ , for all SCs

- 1: For each SC  $n$ , the  $K_{N_b}$  non-coordinated users in cell  $b$  are ranked in descending order according to their SCGs and put in the  $K_{N_b} \times 1$  candidate list  $Pr_{b,n}$
- 2: **while** all of  $N$  SCs and  $K_{N_b}$  non-coordinated users have not been allocated **do**
- 3:   **for** each SC  $n \in [1, N]$  **do**
- 4:     **while**  $\text{sum}(S_{\text{alloc}}(n, :) \neq 0) < L - 1$  **do**
- 5:       From user  $k = 1$  to  $K_{N_b}$  in  $Pr_{b,n}$
- 6:       **if** user  $k$  has not been allocated yet **then**
- 7:          User  $k$  is directly allocated to SC  $n$
- 8:          Set  $S_{\text{alloc}}(n, k) = 1$
- 9:       **else**
- 10:          Assume that user  $k$  has been assigned to other SC (e.g.,  $m$ )
- 11:          **if**  $\hat{H}_{b,k,n} > \hat{H}_{b,k,m}$  **then**
- 12:            According to *Lemma 1*, user  $k$  is allocated to SC  $n$  rather than SC  $m$
- 13:            Set  $S_{\text{alloc}}(n, k) = 1, S_{\text{alloc}}(m, k) = 0$
- 14:            User  $k$  is removed from SC  $m$ 's candidate list
- 15:          **else**
- 16:            User  $k$  is removed from SC  $n$ 's candidate list
- 17:          **end if**
- 18:       **end if**
- 19:     **end while**
- 20:   **end for**
- 21: **end while**

---

*Lemma 1:* In multi-cell coordinated NOMA systems, for the subchannel allocation of non-coordinated users in each BS, the selection of a non-coordinated user with higher SCG leads to less transmission power consumption than any other non-coordinated users with lower SCG on an arbitrary SC.

Based on *Lemma 1*, for each BS, if we select the non-coordinated users with higher SCG on each SC, the network power consumption can be reduced. In light of this, we propose an SCG based subchannel allocation (SCG-SA) algorithm.

1) *SCG-SA for the Non-Coordinated Users:* Since a non-coordinated user is merely served by its serving BS, we perform the subchannel allocation for the non-coordinated users in each cell separately. For BS  $b$  ( $b = 1, \dots, B$ ), since there are  $L - 1$  non-coordinated users served by BS  $b$  to share the same SC with one coordinated user, the number of non-coordinated users in cell  $b$  as  $K_{N_b} = (L - 1)N$ . In SCG-SA, the non-coordinated users are ranked based on their SCGs on each SC by the BS, and the users with higher SCG are more likely to be allocated to this SC. The SCG-SA for the non-coordinated users in cell  $b$  are generalized as follows.

First, for each SC  $n$  ( $n = 1, \dots, N$ ), the  $K_{N_b}$  non-coordinated users are ranked in descending order based on their SCGs on each SC and a  $K_{N_b} \times 1$  candidate list  $Pr_{b,n}$  for non-coordinated users is formed. After that, the  $K_{N_b}$  non-coordinated users are allocated to  $N$  SCs based on these

$$\begin{aligned}
L(\mathbf{P}_n, \mathbf{a}, \mathbf{b}, \mathbf{c}) = & \sum_{b=1}^B \left( \sum_{k=1}^{L-1} p_{u_{bk},n} + p_{u_{BL},n} \right) + \sum_{b=1}^B \left( \sum_{k=1}^{L-1} a_{u_{bk}} (R_{\min} - R_{u_{bk}}) + a_{u_{BL}} (R_{\min} - R_{u_{BL}}) \right) - \\
& \sum_{b=1}^B \left( \sum_{k=1}^{L-1} b_{u_{bk}} p_{u_{bk},n} + b_{u_{BL}} p_{u_{BL},n} \right) + \sum_{b=1}^B \left( \sum_{i=1}^{L-1} \sum_{j=i+1}^{L-2} c_{b,i,j} (p_{u_{bi},n} - p_{u_{bj},n}) + \sum_{i=1}^{L-1} c_{b,i,BL} (p_{u_{bi},n} - p_{u_{BL},n}) \right)
\end{aligned} \quad (20)$$

candidate lists. For each SC  $n$ , from user  $k = 1$  to  $K_{N_b}$  in SC  $n$ ' candidate list  $Pr_{b,n}$ , if the number of users allocated to SC  $n$  is less than  $L - 1$ , user  $k$  is chosen as a candidate user. If user  $k$  has not been allocated yet, it is directly allocated to SC  $n$ . Otherwise, if user  $k$  has already been allocated to other SC (e.g., SC  $m$ ), according to Lemma 1, if the SCGs of user  $k$  on SC  $n$  is larger than that on SC  $m$  (i.e.,  $\hat{H}_{b,k,n} > \hat{H}_{b,k,m}$ ), user  $k$  is allocated to SC  $n$  rather than SC  $m$ , and user  $k$  is removed from the candidate list of the SC  $m$ . Otherwise, user  $k$  is removed from the candidate list of the SC  $n$ .

Repeat these steps until all  $N$  SCs and  $K_{N_b}$  non-coordinated users are allocated. The procedures are presented in Algorithm 1.

2) *SCG-SA for The Coordinated Users*: As mentioned above, the number of coordinated users in the coordinated NOMA system is  $K_C = N$ , with one coordinated user per SC. The SCG-SA for the coordinated users can be briefly described as follows.

First, for each SC  $n$ , the  $K_C$  coordinated users are ranked in descending order based on their SCGs  $\sum_{b \in B_k} \hat{H}_{b,k,n}$ , and a  $K_C \times 1$  candidate list  $Pr_{C,n}$  for coordinated users is formed. After that, the  $K_C$  coordinated users are allocated to the  $N$  SCs based on the candidate lists by the similar approach in Algorithm 1. For each SC  $n$ , the first user (e.g., user  $k$ ) in list  $Pr_{C,n}$  is initially chosen as the candidate user of SC  $n$ . If user  $k$  has not been allocated yet, it is directly allocated to SC  $n$ . Otherwise, if user  $k$  has already been allocated to other SC (e.g., SC  $m$ ), user  $k$  is allocated to the SC with higher SCG and the other SC is rejected. After that, user  $k$  is removed from the candidate list of the rejected SC. Repeat the process above until all  $N$  SCs and  $K_C$  coordinated users are assigned.

## B. Power Allocation

After user mode selection and subchannel assignment, the optimization problem in Eq. (14) can be reformulated as

$$\min_{\mathbf{P}} P_t \quad (18)$$

subject to (C4) – (C6).

Note that constraint (C4) can be rewritten as

( $\widetilde{C4}$ ):

$$\begin{aligned}
p_{k,n} \sum_{b \in B_k} \hat{H}_{b,k,n} + \left( \sum_{b \in B_k} E_{b,k,n} p_{k,n} + \sum_{b \in B_k} (\hat{H}_{b,k,n} + E_{b,k,n}) \right) \\
\sum_{i \in S_{n,b,k}} p_{i,n} + \omega_k \sum_{b \in B_k} (\hat{H}_{b,k,n} + E_{b,k,n}) \sum_{i \in \{S_{n,b}/S_{n,b,k}\}} p_{i,n} + \\
\sum_{b \in \{B/B_k\}} (\hat{H}_{b,k,n} + E_{b,k,n}) \sum_{i \in S_{n,b}} p_{i,n} + \sigma_n^2 \geq 0
\end{aligned}$$

which is a linear inequality with respect to  $\mathbf{P}_n$  to be assigned on SC  $n$ .

Therefore, problem Eq. (18) can be further transformed into

$$\min_{\mathbf{P}} P_t \quad (19)$$

subject to ( $\widetilde{C4}$ ), (C5), (C6),

which is a convex problem. We then attempt to derive the optimal power allocation solution.

As mentioned above, for each SC (e.g., SC  $n$ ), we assume that there are  $L - 1$  non-coordinated users in each cell assigned to share the same SC with one coordinated user. Denote the index of non-coordinated users in each cell  $b$  as user  $u_{b1}, \dots, u_{bL-1}$  ( $b = 1, \dots, B$ ), and the index of the coordinated user as user  $u_{BL}$ . Without loss of generality, we assume  $\hat{H}_{b,u_{b1},n} > \hat{H}_{b,u_{b2},n} > \dots > \hat{H}_{b,u_{BL},n}$ . Since there are  $N$  SCs, define the transmission power matrix as  $\mathbf{P} = [\mathbf{P}_1 \dots \mathbf{P}_n \dots \mathbf{P}_N]^T$ , with  $\mathbf{P}_n = [p_{u_{11},n} \dots p_{u_{1L-1},n} \dots p_{u_{B1},n} \dots p_{u_{BL-1},n} p_{u_{BL},n}]^T$ .

Note that constrains ( $\widetilde{C4}$ ), (C5) and (C6) in Eq. (19) are convex sets, the Lagrange function for SC  $n$  is given in Eq. (20) on the top of this page, with  $\mathbf{a}$ ,  $\mathbf{b}$  and  $\mathbf{c}$  are the Lagrange multiplier matrices.  $\mathbf{a} = [a_{u_{11}} \dots a_{u_{1L-1}} \dots a_{u_{B1}} \dots a_{u_{BL-1}} a_{u_{BL}}]$ ,  $\mathbf{b} = [b_{u_{11}} \dots b_{u_{1L-1}} \dots b_{u_{B1}} \dots b_{u_{BL-1}} b_{u_{BL}}]$ , and  $\mathbf{c} = [c_{1,2,1} \dots c_{1,BL,1} \dots c_{1,BL,L-1} \dots c_{B,2,1} \dots c_{B,BL,1} \dots c_{B,BL,L-1}]$ . Note that all the Lagrange multipliers are not less than 0.

*Lemma 2*: For a coordinated NOMA system with  $B$  BSs, under a minimum rate requirement constraint  $R_{\min}$ , the closed-form solution to power allocation  $\mathbf{P}_n$  on SC  $n$  is

$$\begin{aligned}
\mathbf{P}_n^* = & \left[ p_{u_{11},n}^* \dots p_{u_{1L-1},n}^* \dots p_{u_{B1},n}^* \dots p_{u_{BL-1},n}^* p_{u_{BL},n}^* \right]^T \\
= & \mathbf{A}_n^{-1} \mathbf{Q},
\end{aligned} \quad (21)$$

where  $\mathbf{Q} = [-\alpha \sigma_n^2 \dots -\alpha \sigma_n^2 \dots -\alpha \sigma_n^2]_{1 \times (B(L-1)+1)}^T$ , with  $\alpha = 1 - 2^{R_{\min}}$ .  $\mathbf{A}_n$  is an invertible square matrix with  $((L - 1)B + 1)$  order and can be written in block matrix form as

$$\mathbf{A}_n = \begin{bmatrix} \mathbf{\Lambda}_{11} & \dots & \mathbf{\Lambda}_{1,b} & \dots & \mathbf{\Lambda}_{1,B} & \mathbf{\Lambda}_{1,B+1} \\ \dots & \dots & \dots & \dots & \dots & \dots \\ \mathbf{\Lambda}_{B,1} & \dots & \mathbf{\Lambda}_{B,b} & \dots & \mathbf{\Lambda}_{B,B} & \mathbf{\Lambda}_{B,B+1} \\ \mathbf{\Lambda}_{B+1,1} & \dots & \mathbf{\Lambda}_{B+1,b} & \dots & \mathbf{\Lambda}_{B+1,B} & \mathbf{\Lambda}_{B+1,B+1} \end{bmatrix},$$

where  $\mathbf{\Lambda}_{b,b}$  ( $b = 1, \dots, B$ ) is given on the top of next page and the other block matrices can be expressed as

$$\mathbf{\Lambda}_{b,k} = \begin{bmatrix} \alpha H_{k,u_{b1},n} & \alpha H_{k,u_{b1},n} & \dots & \alpha H_{b,u_{b1},n} \\ \alpha H_{k,u_{b2},n} & \alpha H_{k,u_{b2},n} & \dots & \alpha H_{b,u_{b2},n} \\ \dots & \dots & \dots & \dots \\ \alpha H_{k,u_{bL-1},n} & \alpha H_{k,u_{bL-1},n} & \dots & \alpha H_{b,u_{bL-1},n} \end{bmatrix}_{\substack{(L-1) \times \\ (L-1)}}$$



$$\mathbf{\Lambda}_{b,b} = \begin{bmatrix} \hat{H}_{b,u_{b1},n} + \alpha E_{b,u_{b1},n} & \alpha \omega_{b1} H_{b,u_{b1},n} & \alpha \omega_{b1} H_{b,u_{b1},n} & \dots & \alpha \omega_{b1} H_{b,u_{b1},n} \\ \alpha H_{b,u_{b2},n} & \hat{H}_{b,u_{b2},n} + \alpha E_{b,u_{b2},n} & \alpha \omega_{b2} H_{b,u_{b2},n} & \dots & \alpha \omega_{b2} H_{b,u_{b2},n} \\ \dots & \dots & \dots & \dots & \dots \\ \alpha H_{b,u_{bL-1},n} & \alpha H_{b,u_{bL-1},n} & \alpha H_{b,u_{bL-1},n} & \dots & \hat{H}_{b,u_{bL-1},n} + \alpha E_{b,u_{bL-1},n} \end{bmatrix}_{(L-1) \times (L-1)}$$

$$\mathbf{\Lambda}_{b,B+1} = \begin{bmatrix} \alpha \left( \sum_{i=1, i \neq b}^B H_{i,u_{b1},n} + \omega_{b1} H_{b,u_{b1},n} \right) \\ \alpha \left( \sum_{i=1, i \neq b}^B H_{i,u_{b2},n} + \omega_{b2} H_{b,u_{b2},n} \right) \\ \dots \\ \alpha \left( \sum_{i=1, i \neq b}^B H_{i,u_{bL-1},n} + \omega_{bL-1} H_{b,u_{bL-1},n} \right) \end{bmatrix},$$

$$\mathbf{\Lambda}_{B+1,b} = [\alpha H_{b,u_{BL},n} \quad \dots \quad \alpha H_{b,u_{BL},n}]_{1 \times (L-1)},$$

$$\mathbf{\Lambda}_{B+1,B+1} = \sum_{i=1}^B \left( \hat{H}_{i,u_{BL},n} + \alpha E_{i,u_{BL},n} \right).$$

*Proof of Lemma 2:* See Appendix B.

Now the closed-form of  $\mathbf{P}_n$  is obtained. The transmission power  $P_{t,n}^*$  on SC  $n$  is given by

$$P_{t,n}^* = \sum_{b=1}^B \sum_{k \in S_{n,b}} p_{k,n}^* = \sum_{b=1}^B \left( \sum_{k=1}^{L-1} p_{u_{bk},n}^* + p_{u_{BL},n}^* \right). \quad (22)$$

Hence, the optimal transmission power consumption of the coordinated NOMA system is

$$P_t^* = \sum_{n=1}^N \sum_{b=1}^B \sum_{k \in S_{n,b}} p_{k,n}^* = \sum_{n=1}^N \sum_{b=1}^B \left( \sum_{k=1}^{L-1} p_{u_{bk},n}^* + p_{u_{BL},n}^* \right). \quad (23)$$

## V. LOW-COMPLEXITY FL USER RANKING ORDER BASED JOINT RESOURCE ALLOCATION

The SCG-SA algorithm presented in Section IV provides a feasible subchannel assignment for the coordinated and non-coordinated users. However, it requires user SCG ranking on every SC to form the candidate list, which leads to relatively high complexity. In addition, it lacks a joint subchannel and power allocation, which affects the system performance. It's worth mentioning that if the FL output user ranking list  $\Gamma_{FL}$  generated from user mode selection process can be fed into subchannel and power allocation, the complexity can be dramatically decreased.

In view of this, we propose a FLURO-JRA algorithm in this section, which utilizes the existing FL user ranking list and joint subchannel and power allocation. The proposed FLURO-JRA achieves enhanced performance and requires no extra user ranking in the process of candidate list formation, thus requiring much lower complexity than SCG-SA.

### Algorithm 2 FL User Ranking Order Based Joint Resource Allocation Algorithm

**Require:** Given the  $N \times 1$  list  $P_t = \mathbf{0}$  to record the candidate transmission power on all SCs, and the  $N \times K_C$  allocated list  $S_{\text{alloc2}} = \mathbf{0}$  to record the coordinated users assigned to all SCs

- 1: **for** each cell  $b$  ( $b = 1, \dots, B$ ) **do**
- 2: The candidate list  $Pr_{b,n}$  of every SC  $n$  for the non-coordinated users are formed by FL Ranking List  $\Gamma_{FL}$ .
- 3: Based on the candidate lists, the  $K_{N_b}$  non-coordinated users in cell  $b$  are allocated to  $N$  SCs by using the similar approach in Algorithm 1
- 4: **end for**
- 5: For each SC  $n$ , the candidate list  $Pr_{C,n}$  for the coordinated users is formed by  $\Gamma_{FL}$
- 6: **while**  $\text{rank}(S_{\text{alloc2}}) \neq N$  **do**
- 7: From  $n = 1$  to  $N$ , the first user (e.g., user  $k$ ) in the candidate list  $Pr_{C,n}$  is initially selected
- 8: **if** user  $k$  has not been assigned to other SC yet **then**
- 9: The optimal transmission power  $P_{t,n}^*$  is found by exhaustive search or using Eq. (21)
- 10: Set  $P_t(n, 1) = P_{t,n}^*$ ,  $S_{\text{alloc2}}(n, k) = 1$
- 11: **else**
- 12: Assume user  $k$  has been assigned to SC  $m$ , the optimal transmission power for SC  $n$   $P_{t,n}^*$  is calculated and compared with the candidate transmission power on SC  $m$   $P_t(m, 1)$
- 13: **if**  $P_{t,n}^* < P_t(m, 1)$  **then**
- 14: Set  $S_{\text{alloc2}}(n, k) = 1$ ,  $S_{\text{alloc2}}(m, k) = 0$  and  $P_t(n, 1) = P_{t,n}^*$ ,  $P_t(m, 1) = 0$
- 15: User  $k$  is removed from SC  $m$ 's candidate list
- 16: **else**
- 17: User  $k$  is removed from SC  $n$ 's candidate list
- 18: **end if**
- 19: **end if**
- 20: **end while**

#### A. Algorithm Description

We first concentrate on subchannel assignment for the non-coordinated users. For each cell (e.g., cell  $b$ ), rather than by user SCG ranking, the SCs' candidate lists are directly obtained from the FL user ranking list  $\Gamma_{FL}$ . The  $K_{N_b} \times 1$  candidate list  $Pr_{b,n}$  of every SC  $n$  is formed by extracting the  $K_{N_b}$  non-coordinated users' information in turn from  $\Gamma_{FL}$ , where the users have been previously ranked according to their fuzzy output coordination suitability. After the candidate lists for  $N$  SCs are obtained, the non-coordinated users in each cell are allocated to SCs based on these candidate lists, by

TABLE III  
COMPLEXITY ANALYSIS AND COMPARISON

Algorithms	User Coordination Mode Selection	Subchannel Assignment	Power Allocation
Exhaustive Search	$\mathcal{O}([(B(L-1))N]!)$		$\mathcal{O}((B(L-1))^3 N)$
D-Based User Selection [28] + SCG-SA	$\mathcal{O}((B(L-1))^2 N^2)$	$\mathcal{O}((B(L-1))N^3)$	
CG-Based User Selection [30] + SCG-SA	$\mathcal{O}((B(L-1))^2 N^2)$	$\mathcal{O}((B(L-1))N^3)$	
FL-Based User Selection + SCG-SA	$\mathcal{O}((B(L-1))NB + (B(L-1))^2 N^2)$	$\mathcal{O}((B(L-1))N^3)$	
FL-Based User Selection + FLURO	$\mathcal{O}((B(L-1))NB + (B(L-1))^2 N^2)$	$\mathcal{O}((B(L-1))N + (B(L-1))^3 N)$	

using the similar approach in Algorithm 1.

Now the non-coordinated users in each cell have been assigned. For the coordinated users, similarly, the candidate list  $Pr_{C,n}$  of each SC  $n$  for the coordinated users is formed by the FL ranking list  $\Gamma_{FL}$ . After that, a joint coordinated user subchannel assignment and power allocation scheme is proposed. For each SC  $n$ , the first user (*e.g.*, user  $k$ ) in  $Pr_{C,n}$  is selected as its candidate user. If user  $k$  has not been assigned to other SC, it is directly allocated to SC  $n$  and the optimal transmission power allocation  $P_n^*$  for SC  $n$  is obtained by exhaustive search method or using Eq. (21) and stored as the candidate transmission power of SC  $n$ . Otherwise, assume user  $k$  has already been assigned to another SC (*e.g.*, SC  $m$ ). The optimal transmission power on SC  $n$   $P_n^*$  is found and compared with the candidate transmission power of SC  $m$   $P_t(m, 1)$ . If transmission power consumption of SC  $n$  is lower than that on SC  $m$  ( $P_n^* < P_t(m, 1)$ ), user  $k$  is allocated to the SC  $n$ , rather than SC  $m$ ,  $P_{t,n}^*$  is stored as the candidate transmission power of SC  $n$  and user  $k$  is removed from the candidate list of the SC  $m$ . Otherwise, user  $k$  is removed from the candidate list of the SC  $n$ . The steps above are repeated until all of the  $N$  SCs and  $K_C$  coordinated users are assigned.

The procedures of FLURO-JRA are described in Algorithm 2. After FLURO-JRA, the overall transmission power can be obtained by taking the sum of candidate transmission power on each SC.

### B. Complexity Analysis

The complexity analysis of different schemes is shown in Table III. The optimal user mode selection and subchannel assignment method can only be achieved by exhaustive search of all user combinations and choosing the one which minimizes the transmission power consumption. Given  $K$  users,  $B$  BSs and  $N$  SCs ( $K = (B+1)N$ ), the time complexity of exhaustive search is in the order of  $\mathcal{O}([(B(L-1))N]!)$ . As can be seen from Table III, these schemes provide the same power allocation complexity  $\mathcal{O}((B(L-1))^3 N)$ . Note that for multi-cell coordinated NOMA systems, the number of BSs  $B$  is relatively small (usually 2 or 3 [19]), therefore, the power allocation has much lower complexity than the user mode selection and subchannel assignment. According to the complexity analysis in Table III, it is worth noting that although FL based multi-criterion scheme requires relatively higher complexity than the single-criterion based methods in user mode selection, the complexity of user ranking and subchannel allocation dominates complexity of the whole

algorithm. By utilizing the existing FL user ranking list from user mode selection, FLURO-JRA requires no extra user ranking and has much lower complexity than exhaustive search and the conventional subchannel allocation method based on user ranking in [5] [6].

## VI. NUMERICAL RESULTS AND ANALYSIS

In this section, numerical results are presented to evaluate the performance of our proposed FL based multi-criterion user coordination mode selection and resource allocation algorithms for green coordinated NOMA systems. We consider a two-cell coordinated NOMA, where the radius of each cell is 500 m. The subchannel signal of each user experiences Rayleigh fading, with mean 0 and variance 1. The bandwidth is  $W = 5$  MHz, and  $\sigma_n^2 = \frac{W}{N}N_0$ , with  $N_0 = -174$  dBm/Hz as the noise spectral density. The path loss model is given as a function of distance  $PL(d) = 128.1 + 37.6\log_{10}(d)$  [40], where  $d$  is the distance between the user and an adjacent BS. The circuit power of each BS is  $P_c = 30$  dBm [5]. In addition, we select the user mode selection methods based on a single criterion (*i.e.*, distance [28] or channel gain [30]) as benchmarks.

In Fig. 5, we compare the performance of total transmission power with different user mode selection and resource allocation algorithms, versus the minimum rate requirement  $R_{\min}$ . The number of users is  $K = 9$ , and the number of users sharing in each cell sharing the same SC is  $L = 2$ . As can be seen from Fig. 5, the performance of the proposed FL based multi-criterion user mode selection scheme is substantially better than that of the single-criterion (distance or channel gain) based methods. For example, when shadowing standard deviation is 10 dB and  $R_{\min} = 4$  bps/Hz, the proposed FL based SCG-SA algorithm transmits 36.7% less power than that of traditional single-criterion based SCG-SA methods. The reason is that the FL based user mode selection scheme has considered three parameters including distance, RSRP and VRSRP, which overcomes the drawbacks of the single-criterion based methods and enhances the effectiveness of users' coordination mode selection. In addition, the proposed FLURO-JRA has about 30% less transmission power consumption than the FL based SCG-SA algorithm. That is because FLURO-JRA utilizes a joint subchannel and power allocation scheme and considers the users with high coordination suitability in subchannel allocation. Furthermore, we can also learn from Fig. 5 that the gap of transmission power becomes larger as the shadowing standard deviation

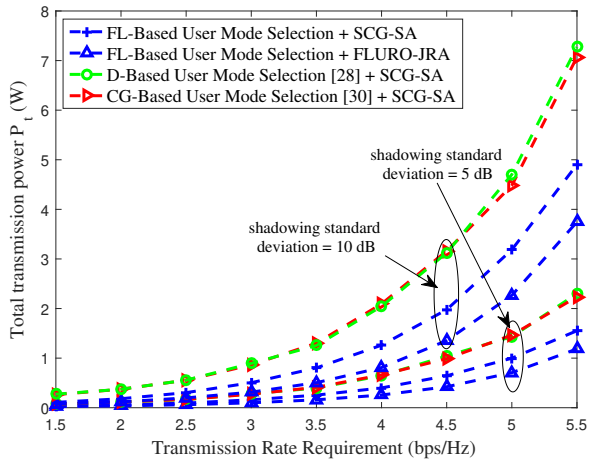


Fig. 5. Transmission power consumption performance for green coordinated NOMA systems under QoS requirement ( $K = 9$ ).

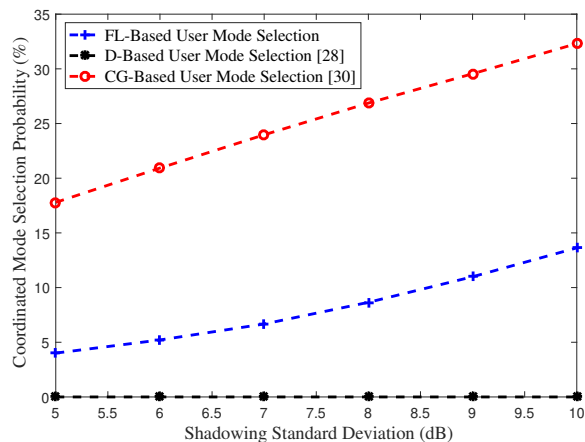


Fig. 6. Coordinated mode selection probability of the users located close to cell center under severe shadowing in multi-cell coordinated NOMA.

increases. That is because the proposed FL based multi-criterion scheme is more effective against fading, shadowing and inter-cell interference than the single-criterion based user mode selection methods, especially when users suffer severe shadowing. This phenomenon can also be proven by Fig. 6, which illustrates the coordinated mode selection probability of users located close to cell center under deep shadowing. Rather than directly choosing the coordinated users by distance [28] or channel gain [30], the FL based user mode selection scheme utilizes FL to balance between the multiple criteria, which improves the effectiveness of user coordination mode selection and achieves a greener coordinated NOMA system.

In Fig. 7, we compare the EE performance of different user mode selection approaches and resource allocation algorithms, with the same constraints of Fig. 5. It can be seen that EE first increases with the increase of  $R_{\min}$ , and then decreases at a certain point. The reason is that there is a tradeoff between total power consumption and users' transmission rate for the power allocation. From this figure, the performance of our

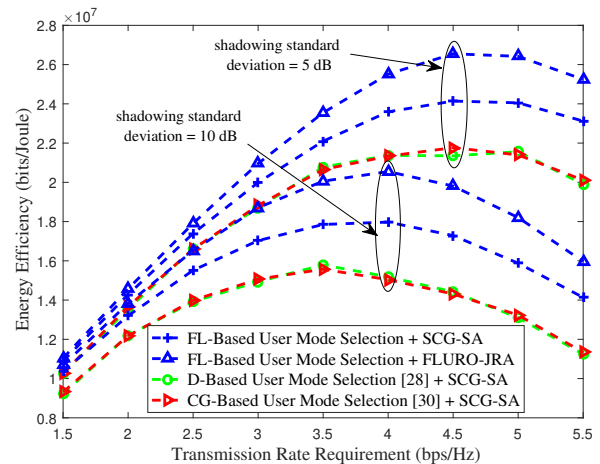


Fig. 7. EE performance for green coordinated NOMA systems under QoS requirement ( $K = 9$ ).

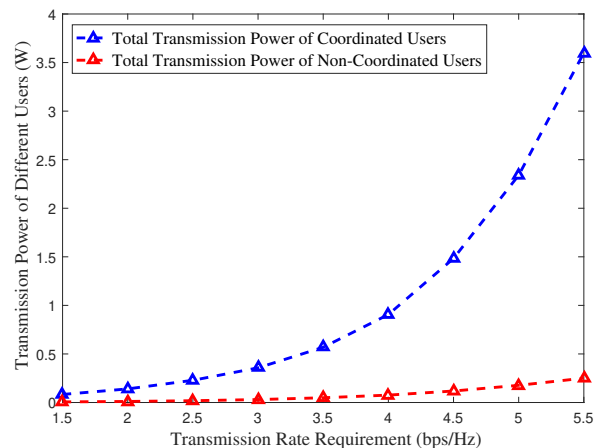


Fig. 8. Transmission power comparison of coordinated and non-coordinated users for FLURO-JRA algorithm ( $K = 9$ ).

proposed FL based SCG-SA and FLURO-JRA algorithms is much more energy-efficient than that of the single-criterion based SCG-SA schemes. In addition, FLURO-JRA achieves better EE performance than the FL based SCG-SA. When shadowing standard deviation is 10 dB and  $R_{\min} = 4.5$  bps/Hz, the EE of FLURO-JRA is 35.3% higher than that of single-criterion based SCG-SA and 14.3% higher than that of FL-based SCG-SA algorithm. The gap of EE becomes larger as  $R_{\min}$  increases. That is because for single-criterion based SCG-SA schemes, more transmission power is allocated to the coordinated users to meet the QoS requirement, which leads to a degradation of EE performance.

Fig. 8 depicts the transmission power of the coordinated users and non-coordinated users with FL based user mode selection and FLURO-JRA algorithm, with the number of users  $K = 9$  and shadowing standard deviation 10 dB. It can be observed from Fig. 8 that the coordinated users require more than 90% of the total transmission power.

Fig. 9 illustrates EE versus the number of users  $K$ , with the QoS requirement  $R_{\min} = 4$  bps/Hz. It can be observed that

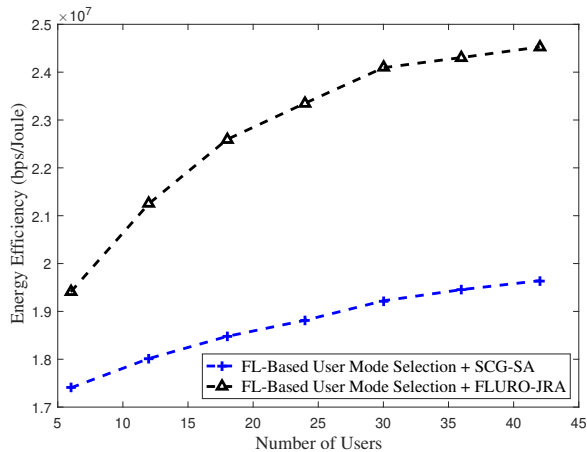


Fig. 9. Impact of the number of users on EE performance for the coordinated NOMA system with  $R_{\min} = 4$  bps/Hz and shadowing standard deviation 10 dB.

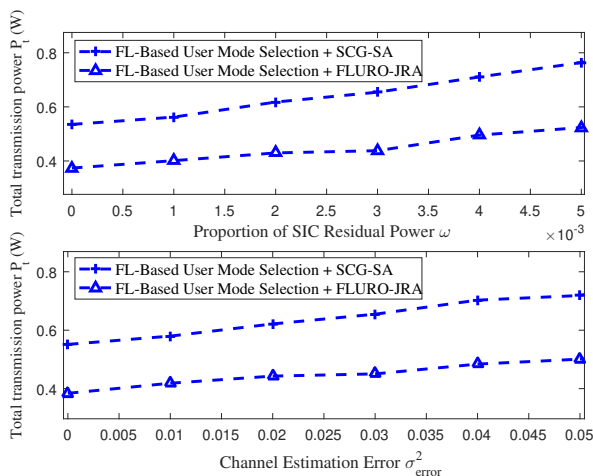


Fig. 10. Impact of imperfect SIC and CSI on the total transmission power for green coordinated NOMA systems with  $R_{\min} = 3$  bps/Hz and shadowing standard deviation 10 dB.

the EE increases with the increase of the number of users, and that the FL based FLURO-JRA significantly outperforms the FL based SCG-SA in terms of EE especially with a larger number of users. When the number of users is  $K = 30$ , the proposed FLURO-JRA has 25% EE improvement over the SCG-SA method.

Fig. 10 shows the total transmission power consumption versus the proportion of SIC residual power  $\omega$ , with perfect CSI  $\sigma_{\text{error}}^2 = 0$ , and the total transmission power consumption versus the CSI estimation  $\sigma_{\text{error}}^2$ , with perfect SIC  $\omega = 0$ , at  $R_{\min} = 3$  bps/Hz. As can be seen, the total transmission power increases slowly with the increase of CSI and SIC errors, demonstrating the robustness of the proposed algorithms.

Fig. 11 shows the performance of the proposed algorithms with exhaustive search, in terms of the total transmission power, with  $K = 6$  users and shadowing standard deviation of 5 dB. It is obvious that with a relatively small number of users, the proposed user mode selection and subchannel assignment algorithms achieve near-optimal performance (the closed-form

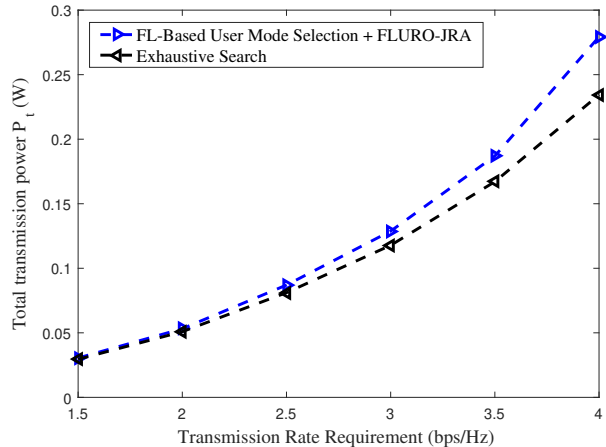


Fig. 11. Performance comparison of the proposed algorithms with exhaustive search with  $K = 6$  users.

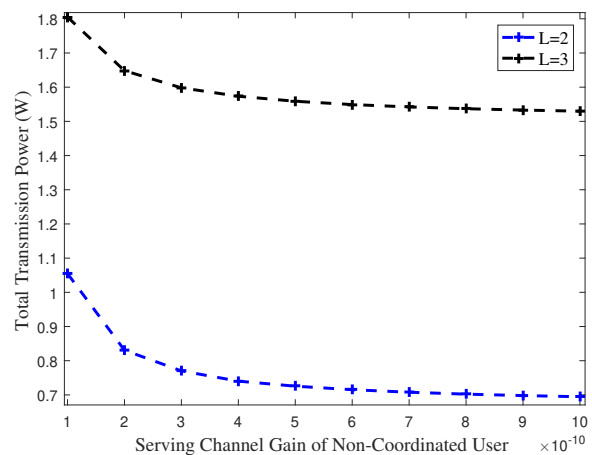


Fig. 12. Illustration of *Theorem 1*: mono-decreasing of the total transmission power with respect to the serving channel gain of the non-coordinated user in each cell with the highest channel gain on the shared SC.

solution to power allocation proposed in Subsection IV-B is optimal), with much less complexity than exhaustive search, as shown in Table III.

Fig. 12 shows the mono-decreasing property of total transmission power with respect to the SCG of the non-coordinated user in a cell with largest channel gain on the shared SC, with the number of users in each cell sharing the same SC as  $L = \{2, 3\}$ ,  $R_{\min} = 4$  bps/Hz,  $N = 1$ . Note that the non-coordinated users usually suffer from poor channel conditions due to the effect of path loss, fading and shadowing, the SCG of non-coordinated user is relatively small. It can be observed from Fig. 12 that the total transmission power monotonically decreases as the SCG of the non-coordinated user continues to increase, which is consistent with *Theorem 1*.

## VII. CONCLUSIONS

In this paper, we have investigated a coordinated NOMA system and proposed an FL based user coordination mode selection algorithm considering multiple criteria of distance,

received signal strength and inter-cell interference, as well as two resource allocation algorithms, SCG-SA and FLURO-JRA, in a multi-subchannel scenario with imperfect CSI and SIC. An intensive analysis of performance and complexity has been provided. FLURO-JRA outperforms SCG-SA and also requires lower complexity than SCG-SA and the algorithms in [5] and [6], thanks to utilizing the FL ranking list for user coordination mode selection, without requiring a separate user ranking process. The proposed multi-criterion based scheme provides superior performance to the single-criterion based methods [28] [30], with transmission power reduction of around 36.7% and EE enhancement of more than 35.3%, thus leading to a greener system. The proposed algorithms provide near-optimal performance with a relatively small number of users, and they are also robust against SIC and CSI errors in a low error range.

#### APPENDIX A PROOF OF THEOREM 1

As mentioned above, for an arbitrary SC (*e.g.*, SC  $n$ ), we assume that there are  $L - 1$  non-coordinated users in each cell assigned to share the same SC with one coordinated user. Denote the index of non-coordinated user allocated to SC  $n$  in cell  $b$  is user  $u_{b1}, \dots, u_{bL-1}$  ( $b = 1, \dots, B$ ), and the index of the coordinated user as user  $u_{BL}$ . Then the SCG of user  $u_{bk}$  can be denoted as  $\hat{H}_{b,u_{bk},n}$ . Without loss of generality, we have  $\hat{H}_{b,u_{b1},n} > \dots > \hat{H}_{b,u_{bL-1},n} > \hat{H}_{b,u_{BL},n}$ .

Taking the partial derivative of the total transmission power with respect to SCG  $\hat{H}_{b,u_{b1},n}$ , we have

$$\frac{\partial P_t}{\partial \hat{H}_{b,u_{b1},n}} = \sum \frac{\partial \mathbf{P}_n}{\partial \hat{H}_{b,u_{b1},n}}. \quad (24)$$

where  $\mathbf{P}_n$  is the power allocation matrix on SC  $n$ . Substituting Eq. (21) into  $\mathbf{P}_n$  yields

$$\frac{\partial \mathbf{P}_n}{\partial \hat{H}_{b,u_{b1},n}} = \frac{\partial \mathbf{A}_n^{-1} \mathbf{Q}}{\partial \hat{H}_{b,u_{b1},n}} = -\mathbf{A}_n^{-1} \frac{\partial \mathbf{A}_n}{\partial \hat{H}_{b,u_{b1},n}} \mathbf{A}_n^{-1} \mathbf{Q}. \quad (25)$$

Since the number of multiplexing users in each SC for each cell  $b$  is  $L$ , the  $(B(L-1)+1) \times (B(L-1)+1)$  matrix  $\mathbf{A}_n$  is given in Eq. (21). Taking the partial derivative of  $\mathbf{A}_n$  with respect to  $\hat{H}_{b,u_{b1},n}$  yields

$$\frac{\partial \mathbf{A}_n}{\partial \hat{H}_{b,u_{b1},n}} = \begin{bmatrix} 0 & \dots & 0 & 0 & \dots & 0 & 0 \dots 0 & 0 \\ \dots & & & & & & & \\ 0 & \dots & 1 & \underbrace{\alpha \omega_{b1} \dots \alpha \omega_{b1}}_{L-2} & \dots & 0 & 0 \dots 0 & \alpha \omega_{b1} \\ \dots & & & & & & & \\ 0 & \dots & 0 & 0 & \dots & 0 & 0 \dots 0 & 0 \end{bmatrix}.$$

Assume the inverse of  $\mathbf{A}_n$  is  $\mathbf{A}_n^{-1} = \frac{\mathbf{D}}{|\mathbf{A}_n|}$ , with  $\mathbf{D}$  as the adjoint matrix, and  $|\mathbf{A}_n|$  as the determinant of  $\mathbf{A}_n$ , respectively. The term  $\sum \frac{\partial \mathbf{P}_n}{\partial \hat{H}_{b,u_{b1},n}}$  can be reformulated as

$$\sum \frac{\partial \mathbf{P}_n}{\partial \hat{H}_{b,u_{b1},n}} = \sum -\mathbf{D} \frac{\partial \mathbf{A}_n}{\partial \hat{H}_{b,u_{b1},n}} \mathbf{D} \mathbf{Q} = (\alpha \sigma_n^2) \times \frac{\left( \sum_{j=1}^{B(L-1)+1} D_{b,j} \right) \left( \sum_{j=1}^{B(L-1)+1} D_{j,b} \right) (1 + (L-1)\alpha \omega_{b1})}{|\mathbf{A}_n|^2}, \quad (26)$$

where  $D_{b,j}$  denotes the  $b$ -th row,  $j$ -th column element of adjoint matrix  $\mathbf{D}$ . Since the value of  $\omega_{b1}$  is assumed to be relatively small, we obtain  $(1 + (L-1)\alpha \omega_{b1}) > 0$ . As a result, the proof of the inequality  $\sum \frac{\partial \mathbf{P}_n}{\partial \hat{H}_{b,u_{bk},n}} < 0$  can be transformed into proving

$$\left( \sum_{j=1}^{B(L-1)+1} D_{b,j} \right) \left( \sum_{j=1}^{B(L-1)+1} D_{j,b} \right) > 0. \quad (27)$$

Notice that in  $\mathbf{A}_n$ , the diagonal element  $\hat{H}_{b,u_{b1},n} + \alpha E_{b,u_{b1},n}$  is the sum of user  $u_{b1}$ 's SCG and channel estimation error multiplied by  $\alpha$ . Given a small number of  $\sigma_{\text{error}}^2$ , we have  $\hat{H}_{b,u_{b1},n} + \alpha E_{b,u_{b1},n} > 0$ . While the non-diagonal elements are the product of users' interference and  $\alpha$ , which are negative.

According to the special structure of  $\mathbf{A}_n$  and the definition of  $\mathbf{D}$ , the diagonal element  $D_{b,b}$  of  $\mathbf{D}$  can be expressed as

$$D_{b,b} = F_{b,0} - \sum_{i=2}^{B(L-1)} (-\alpha)^i F_{b,i}, \quad (28)$$

where  $F_{b,0} = \prod_{i=1}^B \prod_{k=1, u_{ik},n \neq u_{b1}}^{L-1} (\hat{H}_{i,u_{ik},n} + \alpha E_{i,u_{ik},n}) \times \sum_{b=1}^B (\hat{H}_{b,u_{BL},n} + E_{b,u_{BL},n})$  denotes the product of the diagonal elements of  $\mathbf{A}_n$  (except the diagonal element for user  $u_{b1}$ ). The positive terms  $F_{b,i}$ , ( $i = 2, \dots, B(L-1)$ ) stand for the products of different users' SCG, channel estimation error and interference on SC  $n$ .

Similarly, for the non-diagonal elements  $D_{b,j}$  ( $j \neq b$ ), according to the definition of  $\mathbf{A}_n$ , we have

$$D_{b,j} = \sum_{i=1}^{B(L-1)} (-\alpha)^i G_{i,j}, \quad (29)$$

in which the positive terms  $G_{i,j}$  stand for the product of different users' SCG, channel estimation error and interference.

As a result, the term  $\sum_{j=1}^{B(L-1)+1} D_{b,j}$  can be rewritten as

$$\sum_{j=1}^{B(L-1)+1} D_{b,j} = F_{b,0} - \sum_{i=2}^{B(L-1)} (-\alpha)^i F_{b,i} + \sum_{j=1, j \neq b}^{B(L-1)+1} \sum_{i=1}^{B(L-1)} (-\alpha)^i G_{i,j}. \quad (30)$$

Note that for the non-coordinated user  $u_{b1}$  (generally cell-center user), the SCG  $\hat{H}_{b,u_{b1},n}$  from its serving BS  $b$  is much larger than the channel gain from other BSs, *i.e.*,  $\hat{H}_{b,u_{b1},n} \gg \hat{H}_{k,u_{b1},n}$ ,  $k \neq b$ , which implies

$$F_{b,0} \gg F_{b,i}, \quad i = 2, \dots, B(L-1). \quad (31)$$

As a result, we have  $\sum_{j=1}^{B(L-1)+1} D_{b,j} > 0$ . Also, we can prove

$\sum_{j=1}^{B(L-1)+1} D_{j,b} > 0$  by utilizing the same methodology above.

Substituting  $\sum_{j=1}^{B(L-1)+1} D_{b,j} > 0$  and  $\sum_{j=1}^{B(L-1)+1} D_{j,b} > 0$  into Eq. (24) yields

$$\frac{\partial P_t}{\partial \hat{H}_{b,u_{b1},n}} = \sum \frac{\partial \mathbf{P}_n}{\partial \hat{H}_{b,u_{b1},n}} < 0. \quad (32)$$

Hence, we conclude that for coordinated NOMA systems, with relatively low channel estimation error and SIC error, the total transmission power consumption  $P_t$  is mono-decreasing with respect to the SCG of the non-coordinated user in each cell with the highest channel gain on the corresponding SC.

For example, for a two-cell coordinated NOMA system with  $L = 2$ , assume the two non-coordinated users on SC  $n$  are user  $u_{11}$  and  $u_{21}$ , and the index of the coordinated user on SC  $n$  is  $u_{22}$ , respectively. The  $3 \times 3$  matrix  $\mathbf{A}_n$  is

$$\mathbf{A}_n = \begin{bmatrix} \hat{H}_{1,u_{11},n} + \alpha E_{1,u_{11},n} & \alpha H_{2,u_{11}} & \alpha(H_{2,u_{11},n,n} + \omega_{11} H_{1,u_{11},n}) \\ \alpha H_{1,u_{21},n} & \hat{H}_{2,u_{21},n} + \alpha E_{2,u_{21}} & \alpha(H_{1,u_{21},n} + \omega_{21} H_{2,u_{21},n}) \\ \alpha H_{1,u_{22},n} & \alpha H_{2,u_{22},n} & \sum_{i=1}^2 (\hat{H}_{i,u_{22},n} + \alpha E_{i,u_{22},n}) \end{bmatrix}$$

For the non-coordinated user  $u_{11}$  in cell 1, we have

$$\sum \frac{\partial \mathbf{P}_n}{\partial H_{1,u_{11},n}} = \frac{\left( \sum_{b=1}^3 D_{1,b} \right) \left( \sum_{b=1}^3 D_{b,1} \right)}{|\mathbf{A}_n|^2} (\alpha \sigma_n^2),$$

$$D_{1,1} + D_{2,1} + D_{3,1} =$$

$$(\hat{H}_{2,u_{21},n} + \alpha E_{2,u_{21},n}) \sum_{b=1}^2 H_{b,u_{22},n} + \alpha^2 (H_{1,u_{21},n} H_{1,u_{22},n}) +$$

$$(-\alpha) \left( H_{1,u_{21},n} \sum_{b=1}^2 H_{b,u_{22},n} + H_{2,u_{21},n} H_{1,u_{22},n} \right) > 0,$$

$$D_{1,1} + D_{1,2} + D_{1,3} = (\hat{H}_{2,u_{21},n} + \alpha E_{2,u_{21},n}) \sum_{b=1}^2 H_{b,u_{22},n} +$$

$$\alpha^2 (H_{2,u_{11},n} H_{2,u_{22},n} + H_{1,u_{21},n} H_{2,u_{11},n} - H_{1,u_{21},n} H_{2,u_{22},n}) +$$

$$(-\alpha) \left( H_{2,u_{11},n} \sum_{b=1}^2 H_{b,u_{22},n} + H_{2,u_{11},n} H_{2,u_{21},n} \right) > 0,$$

which implies  $\sum \frac{\partial \mathbf{P}_n}{\partial H_{1,u_{11},n}} < 0$ . Similarly, for the other non-coordinated user  $u_{21}$ , we also have  $\sum \frac{\partial \mathbf{P}_n}{\partial H_{2,u_{21},n}} < 0$ . The same result can be obtained as  $B$  increases.

## APPENDIX B PROOF OF LEMMA 2

### A. Analysis of Lagrange Multipliers $\mathbf{a}$ and $\mathbf{b}$

Based on Eq. (20), for all users on SC  $n$  ( $u_{11}, \dots, u_{BL-1}$  and  $u_{BL}$ ), according to the Karush-Kuhn-Tucker (KKT) conditions, we have

$$\frac{\partial L(\mathbf{P}_n, \mathbf{a}, \mathbf{b})}{\partial p_{u_{bk},n}} = 0, \quad (33)$$

$$a_{u_{bk}} (R_{\min} - R_{u_{bk}}) = 0, \quad (34)$$

$$b_{u_{bk}} p_{u_{bk},n} = 0, \quad (35)$$

$$c_{b,i,j} (p_{u_{bi},n} - p_{u_{bj},n}) = 0, \quad (36)$$

with  $i = 1, \dots, L-1, j = i+1, \dots, L-1, BL$ . Then we analyze the range of values for the Lagrange multipliers  $b_{u_{bk}}, c_{b,i,j}$  and  $a_{u_{bk}}$ , respectively.

First, for an arbitrary user  $u_{bk}$  assigned to SC  $n$ , in order to meet the transmission rate requirement  $R_{\min}$ , the transmit power of user  $u_{bk}$  must be greater than 0, i.e.,  $p_{u_{bk},n} > 0$ . Substituting  $p_{u_{bk},n}$  into Eq. (35), we have  $b_{u_{bk}} = 0$ . Similarly, for  $c_{b,i,j}$ , considering a NOMA group with user  $u_{bi}$  and user  $u_{bj}, j = i+1, \dots, L-1, BL$ , since  $i < j$ , we have  $\hat{H}_{b,u_{bi},n} > \hat{H}_{b,u_{bj},n}$ . In order to meet the transmission rate requirement and the principle of NOMA, the transmission power of the two users should satisfy  $p_{u_{bi},n} - p_{u_{bj},n} < 0$  [4] [13]. Substituting  $p_{u_{bi},n} - p_{u_{bj},n} < 0$  into Eq. (36) yields  $c_{b,i,j} = 0$ .

Based on Eq. (20), for a non-coordinated user  $u_{bk}$ , the partial derivative of Lagrange function for SC  $n$   $L(\mathbf{P}_n, \mathbf{a}, \mathbf{b})$  with respect to  $p_{u_{bk},n}$  can be obtained as

$$\frac{\partial L(\mathbf{P}_n, \mathbf{a}, \mathbf{b})}{\partial p_{u_{bk},n}} = 1 - a_{u_{bk}} \frac{\partial R_{u_{bk}}}{\partial p_{u_{bk},n}} - \sum_{i=1}^B \sum_{\substack{j=1, \\ u_{ij} \neq u_{bk}}}^{L-1} a_{u_{ij}} \frac{\partial R_{u_{ij}}}{\partial p_{u_{bk},n}} + \sum_{i=1}^B a_{u_{BL}} \frac{\partial R_{u_{BL}}}{\partial p_{u_{bk},n}}. \quad (37)$$

Substituting  $R_{u_{bk}}$  and  $R_{u_{BL}}$  into Eq. (37) yields

$$\frac{\partial L(\mathbf{P}_n, \mathbf{a}, \mathbf{b})}{\partial p_{u_{bk},n}} = 1 - \frac{a_{u_{bk}} \cdot \partial \gamma_{u_{bk},n} / \partial p_{u_{bk},n}}{(1 + \gamma_{u_{bk},n}) \ln 2} - \sum_{i=1}^B \sum_{\substack{j=1, \\ u_{ij} \neq u_{bk}}}^{L-1} \frac{a_{u_{ij}} \cdot \partial \gamma_{u_{ij},n} / \partial p_{u_{bk},n}}{(1 + \gamma_{u_{bk},n}) \ln 2} - \sum_{i=1}^B \frac{a_{u_{BL}} \cdot \partial \gamma_{u_{BL},n} / \partial p_{u_{bk},n}}{(1 + \gamma_{u_{bk},n}) \ln 2}, \quad (38)$$

where

$$\frac{\partial \gamma_{u_{bk},n}}{\partial p_{u_{bk},n}} = \frac{\hat{H}_{b,u_{bk},n} - E_{b,u_{bk},n}}{(E_{b,u_{bk},n} p_{u_{bk},n} + \sigma_n^2 + I_{u_{bk},n} + \varphi_{u_{bk},n})^2} > 0,$$

and

$$\frac{\partial \gamma_{u_{ij},n}}{\partial p_{u_{bk},n}} = - \frac{p_{u_{ij},n} \hat{H}_{i,u_{ij},n}}{(E_{i,u_{ij},n} p_{u_{ij},n} + \sigma_n^2 + I_{u_{ij},n} + \varphi_{u_{ij},n})^2} \times \left( \frac{\partial I_{u_{ij},n}}{\partial p_{u_{bk},n}} + \frac{\partial \varphi_{u_{ij},n}}{\partial p_{u_{bk},n}} \right), i \neq b, j \neq k.$$

$$\frac{\partial \gamma_{u_{BL},n}}{\partial p_{u_{bk},n}} = - \frac{p_{u_{BL},n} \sum_{i \in B^{u_{BL}}} \hat{H}_{i,u_{BL},n}}{\left( \sum_{i \in B^{u_{BL}}} E_{i,u_{BL},n} p_{u_{BL},n} + \sigma_n^2 + I_{u_{BL},n} + \varphi_{u_{BL},n} \right)^2} \times \left( \frac{\partial I_{u_{BL},n}}{\partial p_{u_{bk},n}} + \frac{\partial \varphi_{u_{BL},n}}{\partial p_{u_{bk},n}} \right).$$

According the definition of the power of intra-cell interference and inter-cell interference in Section II, it is easy to obtain that  $\partial I_{u_{ij},n} / \partial p_{u_{bk},n} \geq 0$ ,  $\partial I_{u_{BL},n} / \partial p_{u_{bk},n} \geq 0$  and  $\partial \varphi_{u_{ij},n} / \partial p_{u_{bk},n} \geq 0$ ,  $\partial \varphi_{u_{BL},n} / \partial p_{u_{bk},n} \geq 0$ , which indicates  $\frac{\partial \gamma_{u_{ij},n}}{\partial p_{u_{bk},n}} \leq 0$  and  $\frac{\partial \gamma_{u_{BL},n}}{\partial p_{u_{bk},n}} \leq 0$ .

Based on Eq. (37), the expression of  $a_{u_{bk}}$  is given by

$$a_{u_{bk}} = \frac{1}{\partial \gamma_{u_{bk},n} / \partial p_{u_{bk},n}} \times \left( (1 + \gamma_{u_{bk},n}) \ln 2 - \sum_{i=1}^B \sum_{\substack{j=1, \\ u_{ij} \neq u_{bk}}}^{L-1} a_{u_{ij}} \cdot \partial \gamma_{u_{ij},n} / \partial p_{u_{bk},n} - \sum_{i=1}^B \frac{a_{u_{BL}} \cdot \partial \gamma_{u_{BL},n} / \partial p_{u_{bk},n}}{(1 + \gamma_{u_{bk},n}) \ln 2} \right).$$

Note that  $a_{u_{ij}} \geq 0$  and  $a_{u_{BL}} \geq 0$ , the term  $\partial\gamma_{u_{ij},n}/\partial p_{u_{bk},n}$  and  $\partial\gamma_{u_{BL},n}/\partial p_{u_{bk},n}$  are negative, for the Lagrange multiplier  $a_{u_{bk}}$  of non-coordinated user  $u_{bk}$ , we obtain

$$a_{u_{bk}} \geq \frac{(1 + \gamma_{u_{bk},n}) \ln 2}{\partial\gamma_{u_{bk},n}/\partial p_{u_{bk},n}} > 0, \quad (39)$$

For the coordinated user  $u_{BL}$ , utilizing the same method above, we can also conclude  $a_{u_{BL}} > 0$ .

### B. A Closed-Form Solution to $\mathbf{P}_n$

As analyzed above, due to the stringent conditions, for the users allocated to SC  $n$ , the Lagrange multiplier matrices should be  $[\mathbf{b}]_{1,k} = 0$ ,  $[\mathbf{c}]_{b,i,j} = 0$ , and  $[\mathbf{a}]_{1,k} > 0$ ,  $k = 1, \dots, B(L-1) + 1$ . As a result, the Lagrange function in Eq. (20) can be rewritten as

$$L(\mathbf{P}_n, \mathbf{a}, \mathbf{b}) = \sum_{b=1}^B \left( \sum_{k=1}^{L-1} p_{u_{bk},n} + p_{u_{BL},n} \right) + \sum_{b=1}^B \left( \sum_{k=1}^{L-1} a_{u_{bk}} (R_{\min} - R_{u_{bk}}) + a_{u_{BL}} (R_{\min} - R_{u_{BL}}) \right), \quad (40)$$

Differentiating  $L(\mathbf{P}_n, \mathbf{a}, \mathbf{b})$  with respect to  $a_{u_{bk}}$  and  $a_{u_{BL}}$ , we have

$$\frac{\partial L(\mathbf{P}_n, \mathbf{a}, \mathbf{b})}{\partial a_{u_{bk}}} = \hat{H}_{b,u_{bk},n} p_{u_{bk},n} + (1 - 2^{R_{\min}}) \times (E_{b,u_{bk},n} + \sigma_n^2 + I_{u_{bk},n} + \varphi_{u_{bk},n}),$$

$$b = 1, \dots, B, k = 1, \dots, L-1.$$

$$\frac{\partial L(\mathbf{P}_n, \mathbf{a}, \mathbf{b})}{\partial a_{u_{BL}}} = p_{u_{BL},n} \sum_{b=1}^B \hat{H}_{b,u_{BL},n} + (1 - 2^{R_{\min}}) \times \left( \sum_{b=1}^B E_{b,u_{BL},n} + \sigma_n^2 + I_{u_{BL},n} + \varphi_{u_{BL},n} \right).$$

Let the equations above equal to zero, we obtain a linear system of  $(B(L-1) + 1)$  equations with  $(B(L-1) + 1)$  unknowns  $\mathbf{P}_n = [p_{u_{11},n} \dots p_{u_{1L-1},n} \dots p_{u_{B1},n} \dots p_{u_{BL-1},n} p_{u_{BL},n}]^T$ .

The  $(B(L-1)+1)$  equations above can be written in matrix form as

$$\begin{bmatrix} \Lambda_{1,1} & \dots & \Lambda_{1,b} & \dots & \Lambda_{1,B} & \Lambda_{1,B+1} \\ & & & & & \\ & & & & & \\ \Lambda_{B,1} & \dots & \Lambda_{B,b} & \dots & \Lambda_{B,B} & \Lambda_{B,B+1} \\ \Lambda_{B+1,1} & \dots & \Lambda_{B+1,b} & \dots & \Lambda_{B+1,B} & \Lambda_{B+1,B+1} \end{bmatrix} \times \begin{bmatrix} p_{u_{11},n} \\ \dots \\ p_{u_{BL-1},n} \\ p_{u_{BL},n} \end{bmatrix} - [-\alpha\sigma_n^2 \dots -\alpha\sigma_n^2 \dots -\alpha\sigma_n^2 \quad -\alpha\sigma_n^2]^T = \mathbf{A}_n \mathbf{P}_n - \mathbf{Q} = \mathbf{0},$$

where  $\Lambda_{11}, \dots, \Lambda_{B+1,B+1}$  have been defined in Section IV-B.

According to the special structure of  $\mathbf{A}_n$  and using the similar methodology in Appendix-A, we can prove  $|\mathbf{A}_n| > 0$ , which indicates matrix  $\mathbf{A}_n$  is invertible.

As a result, by multiplying the inverse of  $\mathbf{A}_n$  on both sides of  $\mathbf{A}_n \mathbf{P}_n = \mathbf{Q}$ , the solution of  $\mathbf{P}_n$  can be obtained as

$$\mathbf{P}_n^* = \mathbf{A}_n^{-1} \mathbf{Q}.$$

## REFERENCES

- [1] L. Dai, B. Wang, Z. Ding, Z. Wang, S. C. and L. Hanzo, "A survey of non-orthogonal multiple access for 5G," *IEEE Communications Surveys & Tutorials*, vol. 20, no. 3, pp. 2294–2323, Sep. 2015.
- [2] Z. Wei, X. Zhu, S. Sun, J. Wang, and L. Hanzo, "Energy efficient full-duplex cooperative non-orthogonal multiple access," *IEEE Transactions on Vehicular Technology*, vol. 67, no. 10, pp. 10123–10128, Aug. 2018.
- [3] S. M. R. Islam, N. Avazov, O. A. Dobre, and K. Kwak, "Power-domain non-orthogonal multiple access (NOMA) in 5G systems: potentials and challenges," *IEEE Communications Surveys & Tutorials*, vol. 19, no. 2, pp. 721–742, Oct. 2016.
- [4] Y. Saito, Y. Kishiyama, A. Benjebbour, E. Cayirci, T. Nakamura, A. Li, and K. Kenichi Higuchi, "Non-orthogonal multiple access (NOMA) for cellular future radio access," in *Proc. IEEE Vehicular Technology Conference (VTC Spring'13)*, Dresden, Germany, Jun. 2013.
- [5] F. Fang, H. Zhang, J. Cheng, and V. C. M. Leung, "Energy-efficient resource allocation for downlink non-orthogonal multiple access network," *IEEE Transactions on Communications*, vol. 64, no. 9, pp. 3722–3732, Jul. 2016.
- [6] W. Cai, C. Chen, L. Bai, Y. Jin, and J. Choi, "Subcarrier and power allocation scheme for downlink OFDM-NOMA systems," *IET Signal Processing*, vol. 11, no. 1, pp. 51–58, Feb. 2017.
- [7] M. Zeng, A. Yadav, O. A. Dobre, G. I. Tsiropoulos, and H. V. Poor, "Capacity comparison between MIMO-NOMA and MIMO-OMA with multiple users in a cluster," *IEEE Journal on Selected Areas in Communications*, vol. 35, no. 10, pp. 2413–2424, Oct. 2017.
- [8] S. Kang, X. Dai, and B. Ren, "Pattern division multiple access for 5G," *Telecommunication Network Technology*, vol. 5, no. 5, pp. 43–47, May 2015.
- [9] Z. Yuan, G. Yu, and W. Li, "Multi-user shared access for 5G," *Telecommunication Network Technology*, vol. 5, no. 5, pp. 28–30, May 2015.
- [10] Y. Du, B. Dong, Z. Chen, J. Fang, and L. Yang, "Shuffled multiuser detection schemes for uplink sparse code multiple access systems," *IEEE Communication Letters*, vol. 20, no. 6, pp. 1231–1234, Jun. 2016.
- [11] D. Fang, Y.-C. Huang, Z. Ding, G. Geraci, S.-L. Shieh, and H. Claussen, "Lattice partition multiple access: A new method of downlink non-orthogonal multiuser transmissions," in *Proc. IEEE Global Communication Conference (GLOBECOM'16)*, Washington DC, USA, Dec. 2016.
- [12] J. Cui, Z. Ding, P. Fan, and N. Al-Dhahir, "Unsupervised machine learning based user clustering in mmWave-NOMA systems," *IEEE Transactions on Wireless Communications*, vol. 17, no. 11, pp. 7425–7440, Sep. 2018.
- [13] Y. Sun, D. W. K. Ng, Z. Ding, and R. Schober, "Optimal joint power and subcarrier allocation for full-duplex multicarrier non-orthogonal multiple access systems," *IEEE Transactions on Communications*, vol. 65, no. 3, pp. 1077–1091, Mar. 2017.
- [14] Y. Liu, M. El-Kashlan, Z. Ding, and G. K. Karagiannidis, "Fairness of user clustering in MIMO non-orthogonal multiple access systems," *IEEE Communications Letters*, vol. 20, no. 7, pp. 1465–1468, Apr. 2016.
- [15] X. Li, C. Li, and Y. Jin, "Dynamic resource allocation for transmit power minimization in OFDM-based NOMA systems," *IEEE Communications Letters*, vol. 20, no. 12, pp. 2558–2561, Sep. 2016.
- [16] W. Hao, Z. Chu, F. Zhou, S. Yang, G. Sun, and K. K. Wong, "Green communication for NOMA-based CRAN," *IEEE Internet of Things Journal*, pp. 1–1, Jul. 2018. (Early Access)
- [17] G. Li, J. Niu, D. Lee, J. Fan, and Y. Fu, "Multi-cell coordinated scheduling and MIMO in LTE," *IEEE Communications Surveys & Tutorials*, vol. 16, no. 2, pp. 761–775, Mar. 2014.
- [18] Y. Sun, Z. Ding, and X. Dai, "On the performance of downlink NOMA in multi-cell mmwave networks," *IEEE Communications Letters*, vol. 22, no. 11, pp. 2366–2369, Nov. 2018.
- [19] M. Ding and H. Luo, *Multi-point cooperative communication systems: theory and applications*. Springer, Berlin, 2013.
- [20] M. S. Ali, E. Hossain, and D. I. Kim, "Coordinated multipoint transmission in downlink multi-cell NOMA systems: models and spectral efficiency performance," *IEEE Wireless Communications*, vol. 25, no. 2, pp. 24–31, Apr. 2018.
- [21] M. Moltafet, R. Joda, N. Mokari, M. R. Sabagh, and M. Zorzi, "Joint access and fronthaul radio resource allocation in PD-NOMA based 5G networks enabling dual connectivity and CoMP," *IEEE Transactions on Communications*, vol. 66, no. 12, pp. 6463–6477, Dec. 2018.

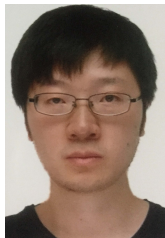
- [22] X. Sun, N. Yang, S. Yan, Z. Ding, D. W. K. Ng, C. Shen, and Z. Zhong, "Joint beamforming and power allocation in downlink NOMA multiuser MIMO networks," *IEEE Transactions on Wireless Communications*, vol. 17, no. 8, pp. 5367–5381, Aug. 2018.
- [23] J. Choi, "Non-orthogonal multiple access in downlink coordinated two-point systems," *IEEE Communications Letters*, vol. 18, no. 2, pp. 313–316, Feb. 2014.
- [24] A. Beylerian and T. Ohtsuki, "Coordinated non-orthogonal multiple access (CO-NOMA)," in *Proc. IEEE Globecom Workshops '16*, Washington DC, USA, Dec. 2016.
- [25] A. G. Armada, R. Corvaja, M. S. Fernandez, and A. S. Rodriguez, "MMSE precoding for downlink coordinated base station transmission," in *Proc. IEEE Vehicular Technology Conference (VTC Spring '11)*, Yokohama, Japan, 2011.
- [26] L. Venturino, A. Zappone, C. Risi, and S. Buzzi, "Energy-efficient scheduling and power allocation in downlink OFDMA networks with base station coordination," *IEEE Transactions on Wireless Communications*, vol. 14, no. 1, pp. 1–14, Jan. 2015.
- [27] O. Munoz, E. Calvo, J. Vidal, and A. Agustin, "Downlink multi-cell radio resource management for coordinated base stations," in *Proc. IEEE Vehicular Technology Conference (VTC Spring '09)*, Barcelona, Spain, Apr. 2009.
- [28] Z. Liu, G. Kang, L. Lei, N. Zhang, and S. Zhang, "Power allocation for energy efficiency maximization in downlink CoMP systems with NOMA," in *Proc. IEEE Wireless Communications and Networking Conference (WCNC '17)*, San Francisco, CA, USA, May 2017.
- [29] J. Lee, Y. Kim, H. Lee, B. Ng, D. Mazzaresse, J. Liu, W. Xiao, and Y. Zhou, "Coordinated multipoint transmission and reception in LTE-Advanced systems," *IEEE Communications Magazine*, vol. 50, no. 11, pp. 44–50, Nov. 2012.
- [30] Y. Tian, A. Nix, and M. Beach, "On the performance of opportunistic NOMA in downlink CoMP networks," *IEEE Communication Letters*, vol. 20, no. 5, pp. 998–1001, Mar. 2016.
- [31] Q. Zhang and C. Yang, "Transmission mode selection for downlink coordinated multipoint systems," *IEEE Transactions on Vehicular Technology*, vol. 62, no. 1, pp. 456–471, Sep. 2013.
- [32] J. Qadir, K. A. Yau, M. A. Imran, Q. Ni, and A. V. Vasilakos, "IEEE access special section editorial: artificial intelligence enabled networking," *IEEE Access*, vol. 3, pp. 3079–3082, 2015.
- [33] T. J. Ross, *Fuzzy Logic with Engineering Applications*. John Wiley and Sons, Chichester, 2004.
- [34] A. Niemi, J. Joutsensalo, and T. Ristaniemi, "Fuzzy channel estimation in multipath fading CDMA channel," in *Proc. IEEE International Symposium on Personal Indoor and Mobile Radio Communications (PIMRC'00)*, London, UK, Sep. 2000, vol. 2, pp. 1131–1135.
- [35] P. Munoz, R. Barco, and I. Bandera, "On the potential of handover parameter optimization for self-organizing networks," *IEEE Transactions on Vehicular Technology*, vol. 62, no. 5, pp. 1895–1905, Feb. 2013.
- [36] Y. Wang, D. Wang, J. Pang, and G. Shen, "Self-optimization of downlink transmission power in 3GPP LTE-A heterogeneous network," in *Proc. IEEE Vehicular Technology Conference (VTC-Fall '12)*, Quebec City, QC, Canada, Sep. 2012.
- [37] X. Zhu and R. D. Murch, "Performance analysis of maximum likelihood detection in a MIMO antenna system," *IEEE Transactions on Communications*, vol. 50, no. 2, pp. 187–191, Feb. 2002.
- [38] X. Yan, J. Ge, Y. Zhang, and L. Gou, "NOMA-based multiple-antenna and multiple relay networks over Nakagami-m fading channels with imperfect CSI and SIC error," *IET Communications*, vol. 12, no. 17, pp. 2087–2098, Oct. 2018.
- [39] P. Huang and Y. Pi, "A novel MIMO channel state feedback scheme and overhead calculation," *IEEE Transactions on Communications*, vol. 16, no. 10, pp. 4550–4562, Oct. 2018.
- [40] *Further Advancements for E-UTRA Physical Layer Aspects*. 3GPP TR 36.814 V9.0.0, Mar. 2010. Available: [http://www.3gpp.org/ftp/Specs/archive/36\\_series/36.814/](http://www.3gpp.org/ftp/Specs/archive/36_series/36.814/)



**Haiyong Zeng** (S'18) received his B.S. and M.S. degrees in Control Theory and Engineering from Chongqing University of Posts and Telecommunications, Chongqing, China, in 2013 and 2016, respectively. He is currently pursuing the Ph.D. degree with the School of Electrical and Information Engineering, Harbin Institute of Technology, Shenzhen, China. His research interests include green communications, wireless communication systems and protocols and wireless resource allocation.



**Xu Zhu** (S'02-M'03-SM'12) received the B.Eng. degree (Hons.) in electronics and information engineering from the Huazhong University of Science and Technology, Wuhan, China, in 1999, and the Ph.D. degree in electrical and electronic engineering from The Hong Kong University of Science and Technology, Hong Kong, in 2003. She joined the Department of Electrical Engineering and Electronics, University of Liverpool, Liverpool, UK, in 2003, as an Academic Member, where she is currently a Reader. She has over 160 peer-reviewed publications on communications and signal processing. Her research interests include MIMO, channel estimation and equalization, resource allocation, cooperative communications, and green communications. She has acted as a Chair for various international conferences, such as the Vice-Chair of the 2006 and 2008 ICARN International Workshops, the Program Chair of ICSAI 2012, the Symposium Co-Chair of the IEEE ICC 2016 and 2019, and the Publicity Chair of the IEEE IUC 2016. She has served as an Editor for the *IEEE TRANSACTIONS ON WIRELESS COMMUNICATIONS* and a Guest Editor for several international journals such as *Electronics*.



search interests include Li-Fi, synchronization, full-duplex, and blind source separation.

**Yufei Jiang** (S'12-M'14) received the Ph.D. degree in electrical engineering and electronics from the University of Liverpool, Liverpool, UK, in 2014. From 2014 to 2015, he was a Post-Doctoral Researcher with the Department of Electrical Engineering and Electronics, University of Liverpool. From 2015 to 2017, he was a Research Associate with the Institutes for Digital Communications, University of Edinburgh, Edinburgh, UK. He is currently an Assistant Professor with the Harbin Institute of Technology, Shenzhen, China. His research



interests include constructive interference design, green communications, full-duplex, millimeter-wave communications and algorithm design. He was the recipient of the Graduate China National Scholarship Award in 2012, the recipient of the A\*STAR Research Attachment Programme (ARAP) Studentship in 2016, and the recipient of the CSC Outstanding Self-Financed Scholarship in 2017.

**Zhongxiang Wei** (S'15-M'17) received the Ph.D. degree in electrical engineering and electronics from the University of Liverpool, Liverpool, UK, in 2017. From March 2016 to March 2017, he was with the Institution for Infocomm Research, Agency for Science, Technology, and Research, Singapore, as a research assistant. From March 2017 to October 2017, he was a visiting student with the Wireless Networks and Communications Group, Harbin Institute of Technology, Shenzhen, China. Since early 2018, he has been working with the University College London (UCL), London, as a research associate. His research interests



include sensor networks, cooperative communications, adaptive filtering, and resource optimization.

**Tong Wang** (S'10-M'12) received the B.Eng. degree in electrical engineering and automation from Beijing University of Aeronautics and Astronautics (current name: Beihang University), Beijing, China, in 2006 and the M.Sc. degree (with distinction) in communications engineering and the Ph.D. degree in electronic engineering from the University of York, York, UK, in 2008 and 2012, respectively.

From 2012 to 2015, he was a Research Associate with the Institute for Theoretical Information Technology, RWTH Aachen University, Aachen, Germany. From 2014 to 2015, he was a Research Fellow of the Alexander von Humboldt Foundation. Since March 2016, he has been with the Department of Electronic and Information Engineering, Harbin Institute of Technology, Shenzhen, China, where he is an Assistant Professor. His research interests